

Report

**P-17-11**

August 2017



# Surface morphology and elemental composition of copper canisters for disposal of spent nuclear fuel

**Carl-Johan Högberg**

**Oskar Karlsson**

**Mats Randelius**

**Adam Johannes Johansson**

SVENSK KÄRNBRÄNSLEHANTERING AB

SWEDISH NUCLEAR FUEL  
AND WASTE MANAGEMENT CO

Box 3091, SE-169 03 Solna  
Phone +46 8 459 84 00  
skb.se

SVENSK KÄRNBRÄNSLEHANTERING



ISSN 1651-4416

**SKB P-17-11**

ID 1582083

August 2017

# **Surface morphology and elemental composition of copper canisters for disposal of spent nuclear fuel**

Carl-Johan Högberg, Oskar Karlsson, Mats Randelius  
Swerea KIMAB

Adam Johannes Johansson  
Svensk Kärnbränslehantering AB

Data in SKB's database can be changed for different reasons. Minor changes in SKB's database will not necessarily result in a revised report. Data revisions may also be presented as supplements, available at [www.skb.se](http://www.skb.se).

A pdf version of this document can be downloaded from [www.skb.se](http://www.skb.se).

© 2017 Svensk Kärnbränslehantering AB



## Summary

The surface morphology and elemental composition of samples from unexposed copper tubes, made of the same material type and manufacturing process as for the test *in situ* series Prototyp repository, ongoing in the Äspö Hard Rock Laboratory (HRL), has been studied using optical microscopy, scanning electron microscopy, energy dispersive spectroscopy and glow discharge optical emission spectroscopy. From the analysis it can be concluded that there are occasional pits and cracks that are a few  $\mu\text{m}$  deep. Besides copper, oxygen and carbon are the main elements close to the surface. Some hydrogen has been detected within the first  $\mu\text{m}$  from the surface. The surface is contaminated with carbon, sulphur, chlorine and other elements.



# Contents

<b>1</b>	<b>Background</b>	7
<b>2</b>	<b>Investigation</b>	9
2.1	Samples and sample preparation	9
2.2	Optical microscopy	9
2.3	Scanning electron microscopy (SEM) and energy dispersive spectroscopy (EDS) analysis	9
2.4	Glow discharge – optical emission spectroscopy (GD-OES)	9
<b>3</b>	<b>Results</b>	11
3.1	Microscopical examination	11
3.2	Scanning electron microscopy	15
3.3	EDS mapping	23
3.4	GD-OES analysis	27
<b>4</b>	<b>Discussion</b>	31
<b>5</b>	<b>Conclusion</b>	33
	<b>References</b>	35
	<b>Appendix A</b> Additional photos	37





# 1 Background

Surfaces of unexposed copper tubes made of oxygen free phosphorous doped (OFP) copper, has been examined regarding surface morphology and surface elemental composition, in order to be compared with results obtained from copper canisters of the *in situ* test series Prototype repository (Taxén et al. 2012, Taxén 2013). The full-scale copper canisters in the Prototype series were exposed initially to the oxygen saturated bentonite pore water and later to the anoxic saline ground water in Äspö Hard Rock Laboratory (HRL) for more than eight years. Furthermore, the canisters of the Prototype series were heated to around 35°C. In comparison, the material examined herein was exposed only to the relatively dry indoor environment at SKB's Canister Laboratory in Oskarshamn. Examination of copper material manufactured at the same time and with the same method as the copper canisters exposed to the ground water in the Prototype test, can give an idea of what the material looked like before the exposure in Äspö HRL.



## 2 Investigation

### 2.1 Samples and sample preparation

An extruded copper tube denoted T30 with manufacturing date 2001-12 has been chosen as sample material, since it is considered to be equivalent to the material used to extrude the copper tubes T28 and T29, used to manufacture the full-scale canisters of the Prototype series (manufacturing date 2001-03). After manufacturing and machining, the material has been stored in a dry indoor environment at SKB's canister lab in Oskarshamn. Two samples with a diameter of 4 cm were core drilled by SKB from the tube. The sample denoted A was taken from a part of the surface that appeared visually darker, while the sample denoted B was taken from a lighter area. The two samples were sent to Swerea KIMAB in Kista for metallographic examination.

Cross sections of samples A and B were compression mounted in Buehler Konductomet compound. The specimens are oriented so that the surface profile of the external surface of the copper tube could be studied. The samples were grinded, using a rotating disc with abrasive paper, to a fineness of 4000. Thereafter, the samples were polished with diamond paste from 3  $\mu\text{m}$  down to 0.25  $\mu\text{m}$ . These samples were used for analysis in a scanning electron microscope.

Two other cross sections of A and B were prepared as described above but were also etched to make the microstructure visible. The etchant used was 40 g  $\text{CrO}_3$ , 7.5 g  $\text{NH}_4\text{Cl}$ , 50 ml concentrated  $\text{H}_2\text{SO}_4$ , 50 ml concentrated  $\text{HNO}_3$  and 1900 ml  $\text{H}_2\text{O}$ . The samples were dipped for about 5 s and then washed in water and then in ethanol.

Energy dispersive spectroscopy mapping and glow discharge optical emission spectroscopy was performed directly on the sample surfaces.

### 2.2 Optical microscopy

Overview images were obtained with a Zeiss Axio Zoom V16. Magnified images were taken with a Nikon Epiphot equipped with a digital camera Kappa DX40. Measurements in the z-axis were made using a calibrated focus knob.

### 2.3 Scanning electron microscopy (SEM) and energy dispersive spectroscopy (EDS) analysis

SEM images were obtained with a Zeiss Supra scanning electron microscope with a field emission gun (FEG) as electron source. The energy was 15 keV for the electron beam and the working distance about 10 mm. The detector for backscattered electrons was used. The microscope is equipped with a detector for energy dispersive spectrometry (EDS) which was used for elemental analysis in small areas and for EDS-mapping of the sample surfaces.

### 2.4 Glow discharge – optical emission spectroscopy (GD-OES)

GD-OES was used in order to obtain a depth profile of the elemental composition. The instrument used was a Leco 850A glow discharge spectrometer. For the profile measurements performed, the detection limit is estimated as 0.1% and the accuracy would be one or a few %.

Calibration was carried out using reference materials (RM) initially of aluminium (1257), brass (2161-5), titanium-hydride ( $\text{TiH}_2$ ), ceramic (Ker1), stainless steel (SDN-71), aluminium-silicon (ST4), and cast iron (C1145A). Thereafter a final calibration was carried out using several copper reference materials of varying qualities (Cu0X, Cu Hög, C1253). Cu0X and Cu Hög are in-house reference materials of pure and doped copper.



## 3 Results

### 3.1 Microscopical examination

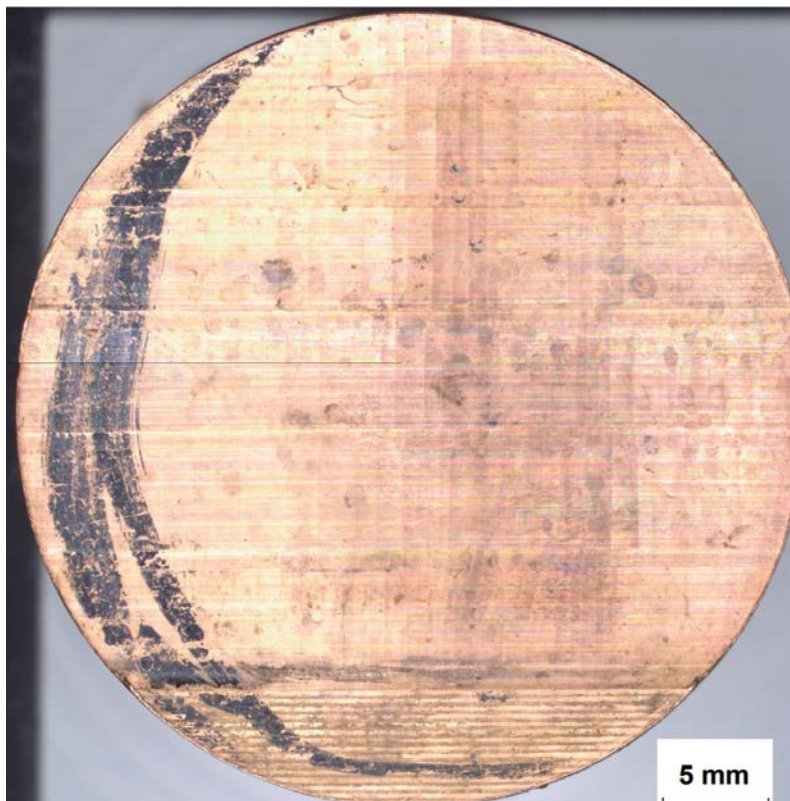
In Figure 3-1 an overview image of the surface of sample A is shown. The main part of the surface has a pattern with vertical lines. The bottom part is however different with more coarse horizontal lines.

In Figure 3-2 images from different areas on sample A are shown. A1–A3 show deposits on the surface, indicated with arrows. The thickness of the deposits in A1 was too small to be measured in the microscope ( $< 1 \mu\text{m}$ ). In A2, the deposits were about  $1 \mu\text{m}$  thick and in A3  $5 \mu\text{m}$ . A4 and A5 show the vertical lines that can be seen in the overview image in Figure 3-1. The lines are channels, so shallow that they could not be measured. A6 shows a magnification of the horizontal pattern at the bottom of the sample in Figure 3-1. It is about  $0.25 \text{ mm}$  between the traces and they are  $3 \mu\text{m}$  deep.

In Figure 3-3 an overview image over the surface of sample B is shown. The appearance with equidistant lines (channels) is the same over the whole surface.

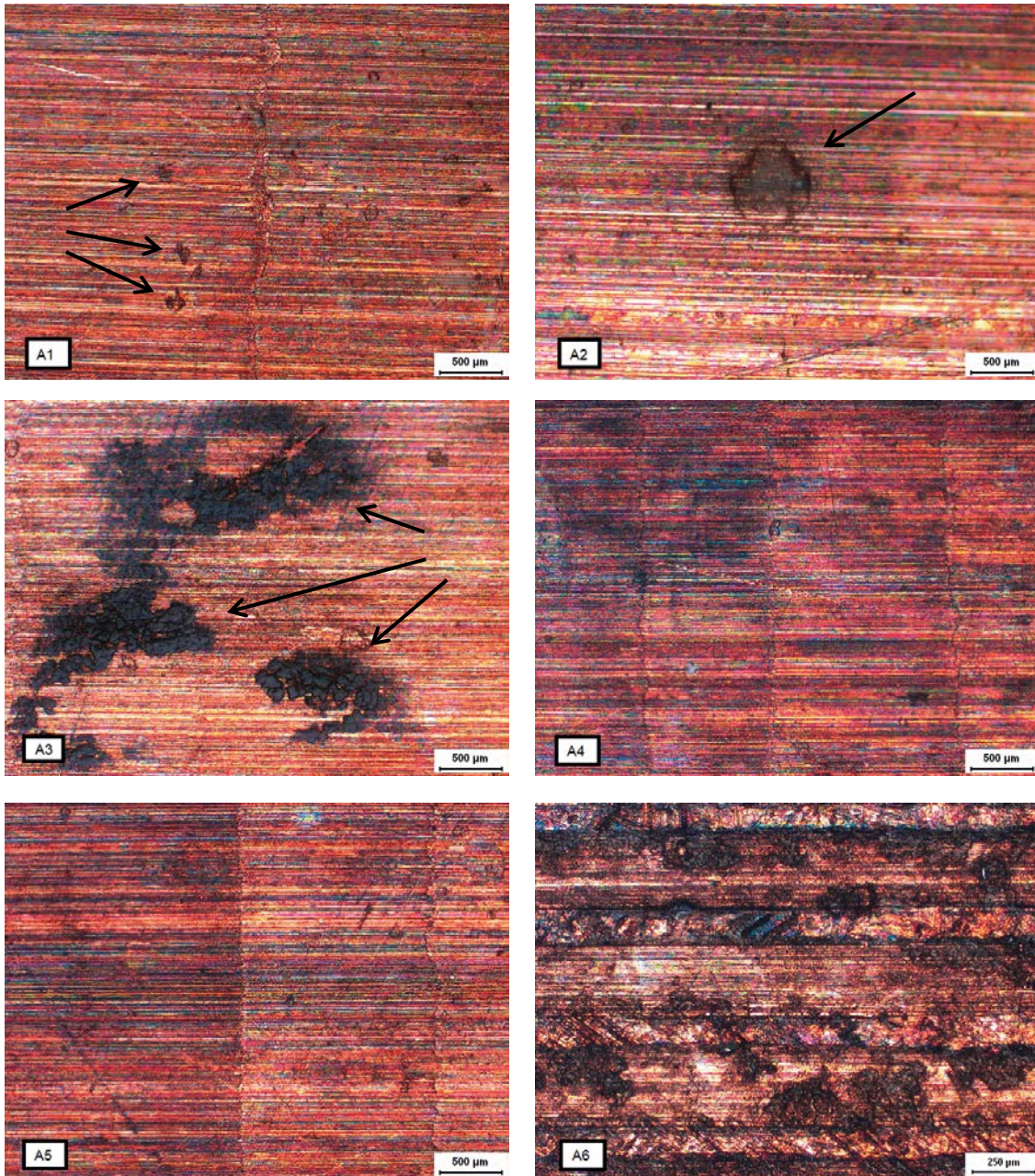
In Figure 3-4, magnifications of the surface for sample B is shown. B1 and B2 are magnifications of the pattern visible in the overview image in Figure 3-3. In B2, the depth of the channels was measured to  $2 \mu\text{m}$ . The thickness of the deposit in B3 is up to  $10 \mu\text{m}$  and up to  $13 \mu\text{m}$  in B4. The deposits are indicated with arrows.

Figure 3-5 to Figure 3-8 show images of cut parts of the samples, which were etched in order to see the microstructure.



**Figure 3-1.** Overview for the surface of the core drilled sample A as received before any sample preparation was made.





**Figure 3-2.** Magnifications of the surface of sample A with arrows indicating deposits. The scale bars are 500  $\mu\text{m}$  for A1–A5 and 250  $\mu\text{m}$  for A6.



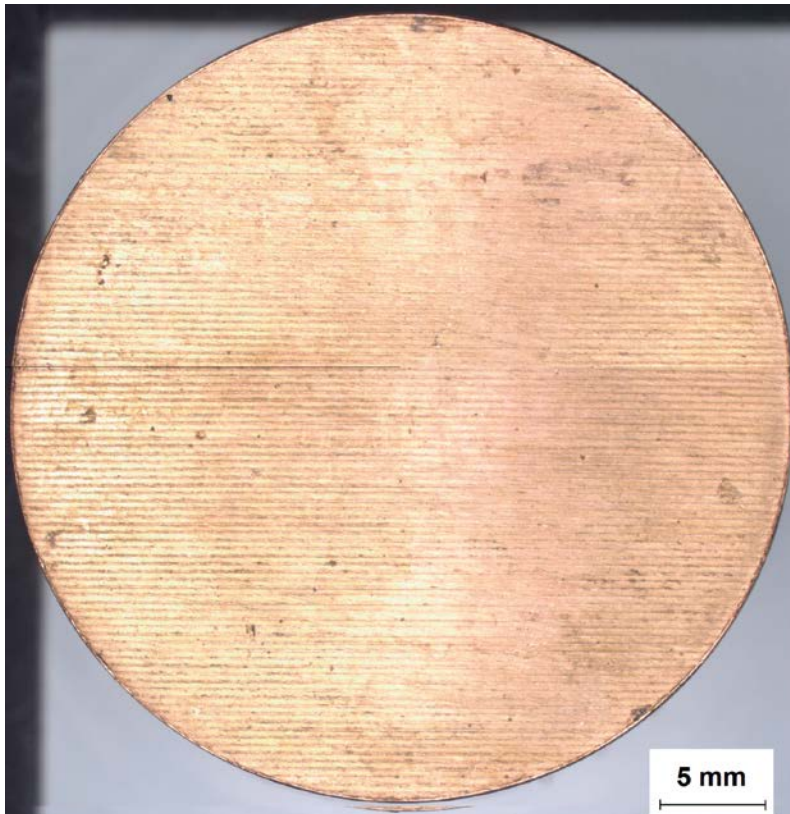


*Figure 3-3. Overview image of the surface of core drilled sample B as received before any sample preparation was made.*

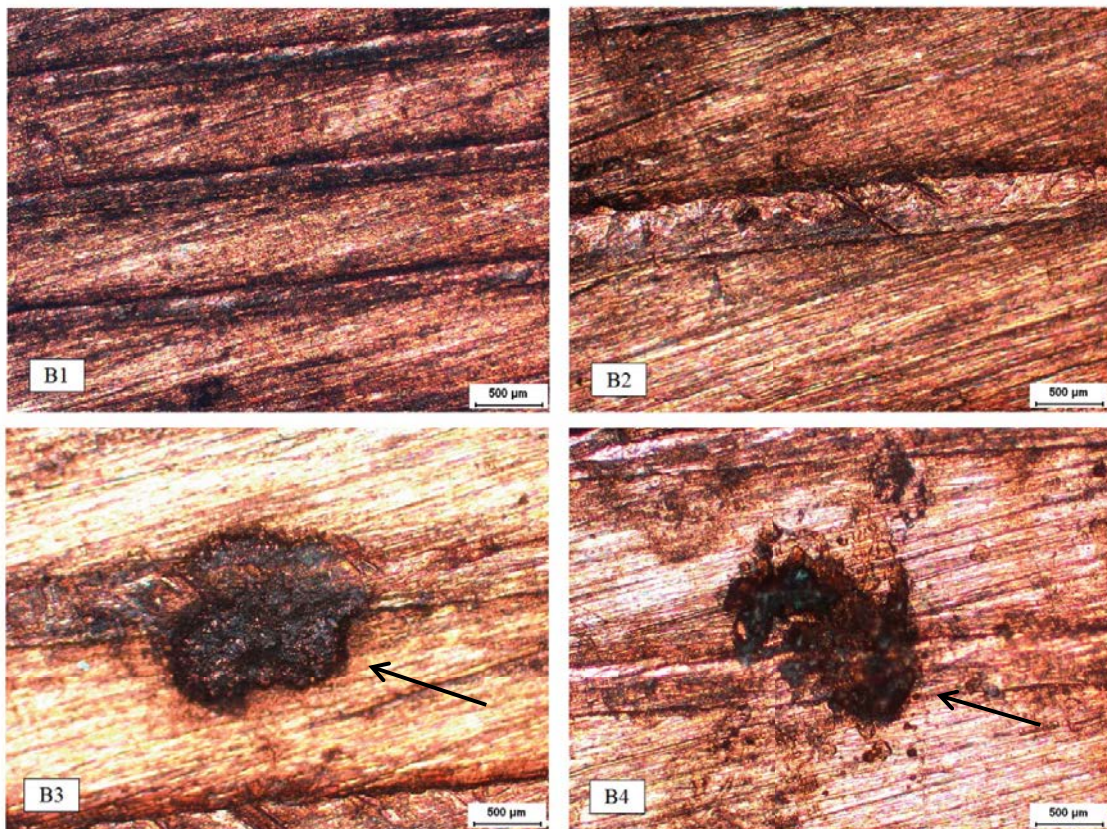


*Figure 3-4. Magnification of the surface of sample B with arrows indicating deposits. The scale bars are 500  $\mu\text{m}$ .*



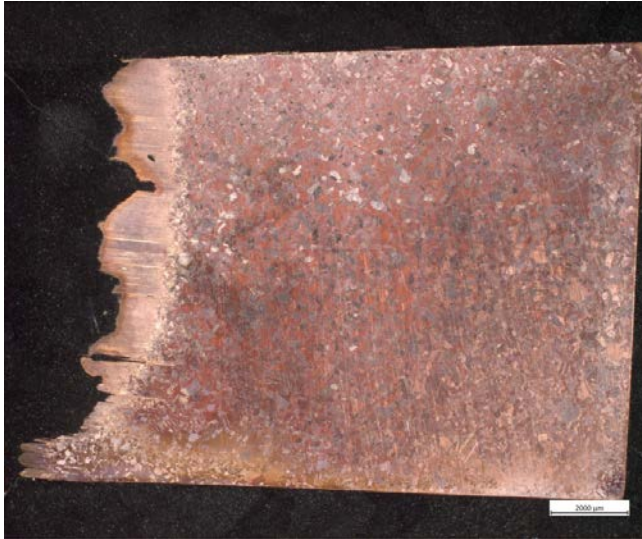


**Figure 3-5.** Overview image of etched sample for A. The scale bar is 2 mm.

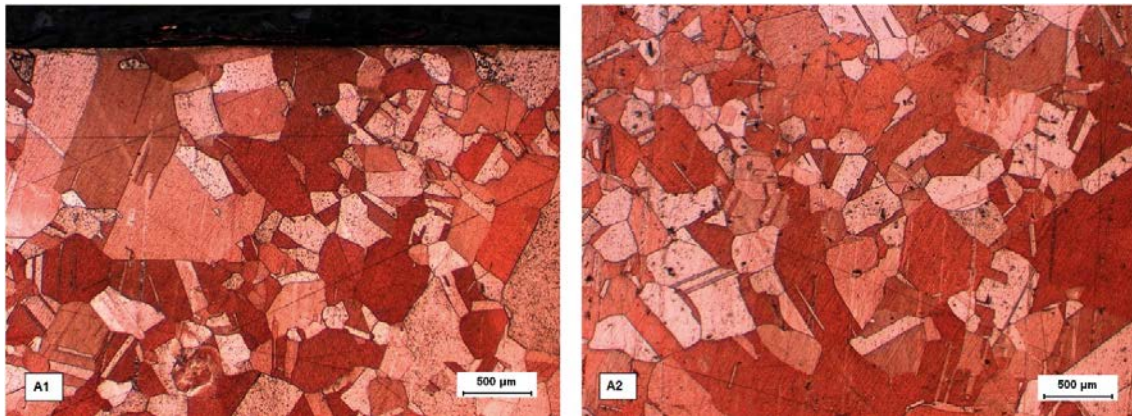


**Figure 3-6.** Metallographic cross section of sample A. A1 shows the area close to the surface and A2 further into the bulk of the sample. The scale bars are 500 μm.

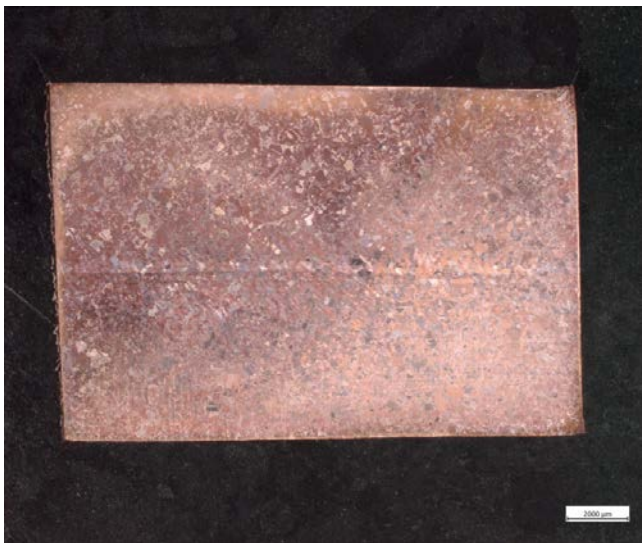


**Figure 3-7.** Overview image of etched sample for B. The scale bar is 2 mm.



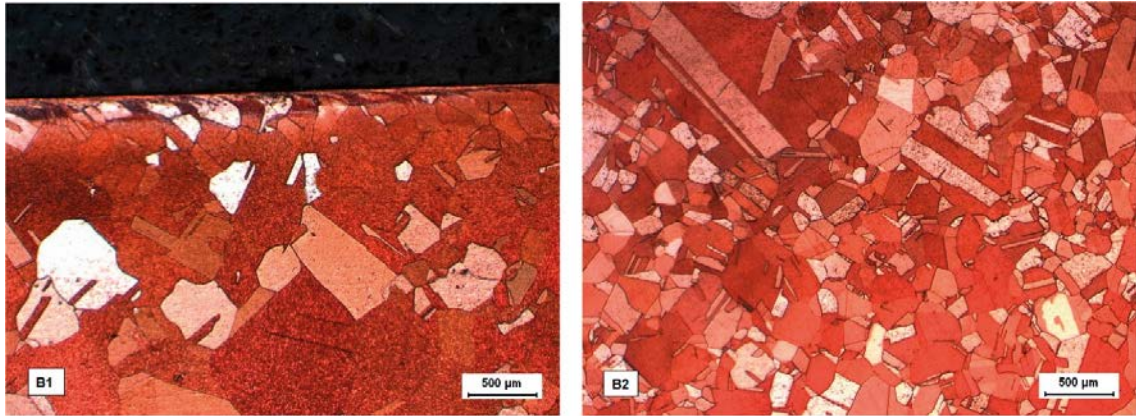


**Figure 3-8.** Metallographic cross section of sample B. B1 shows the area close to the surface and B2 further into the bulk of the sample. The scale bars are 500 µm.

### 3.2 Scanning electron microscopy

A selection of the SEM-images is shown below. Additional SEM-images are included in Appendix A. In Figure 3-9 to Figure 3-15, different images of the surface profile of sample A are shown and in Figure 3-16 to Figure 3-20, different images of the surface profile of sample B. For some of the images, EDS analysis has been made in pits. These results are shown right after each SEM image in Table 3-1 to Table 3-4.

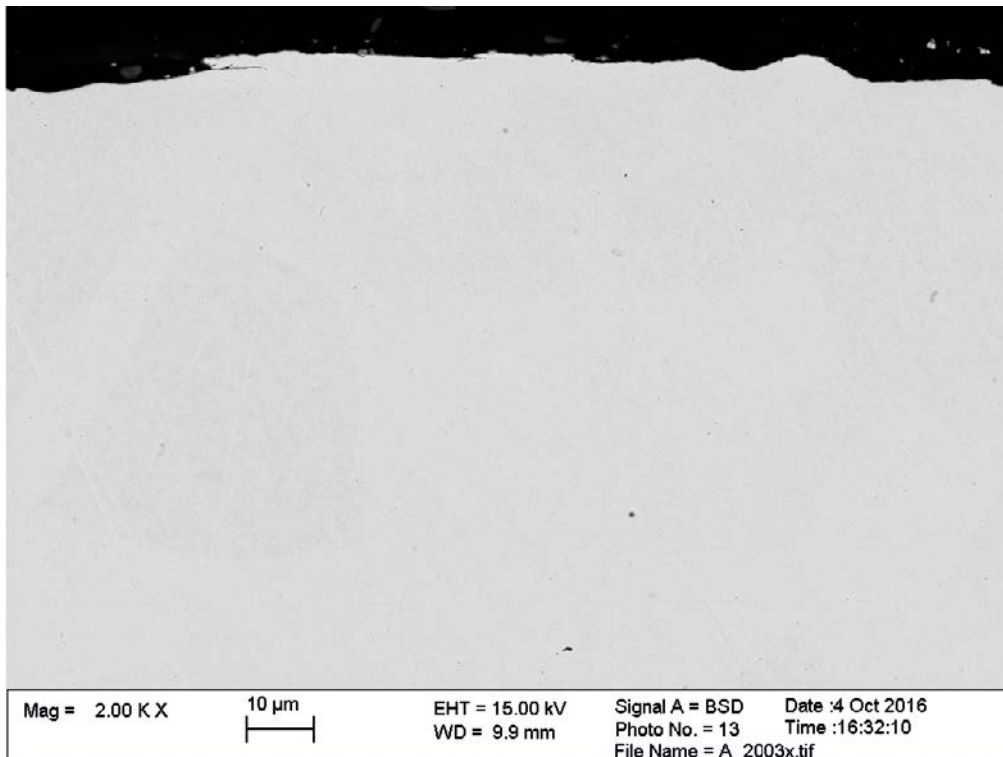


**Figure 3-9.** Surface profile of sample A.

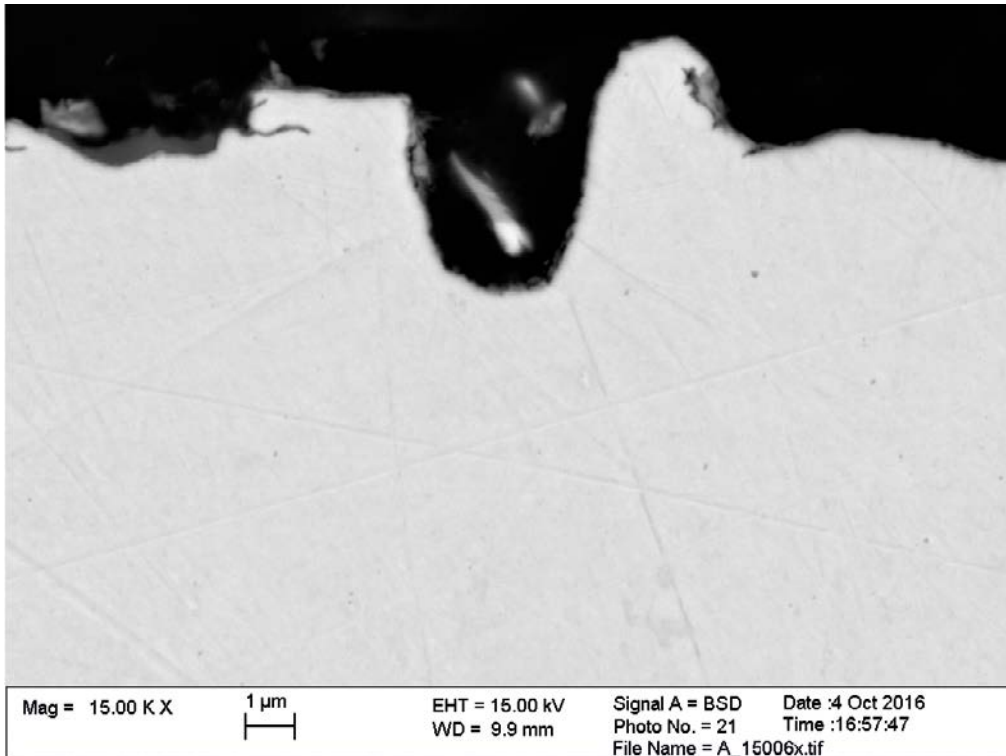


*Figure 3-10. The deepest pit that could be found on sample A, about 3  $\mu$ m deep.*

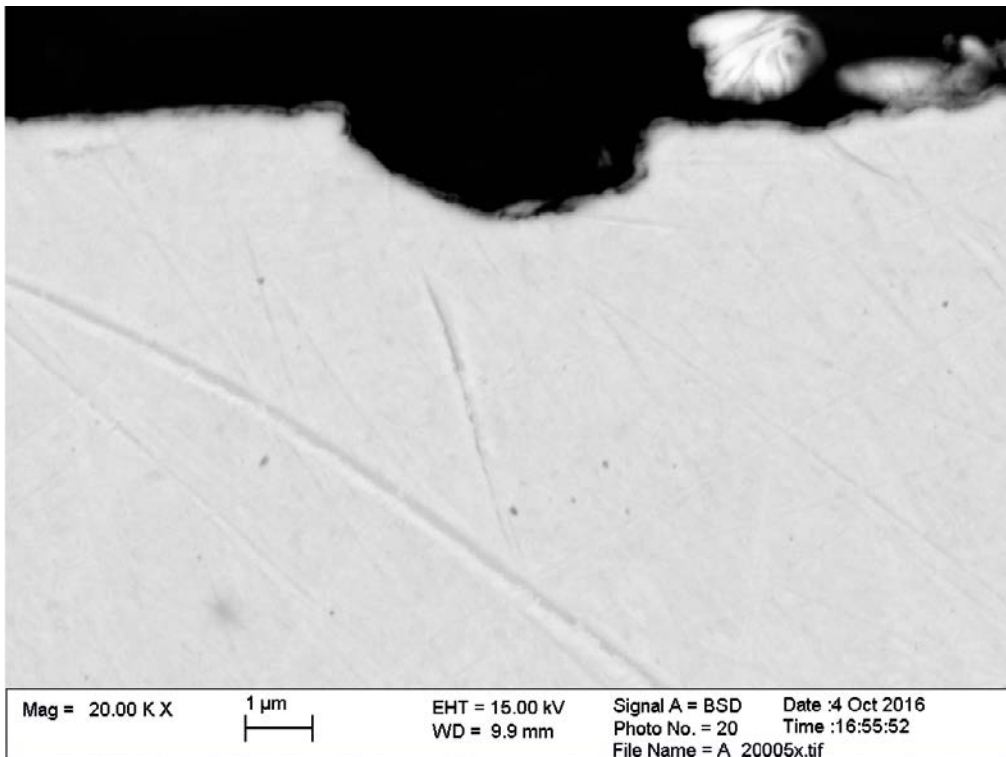


*Figure 3-11. About 1  $\mu$ m deep pit on sample A.*

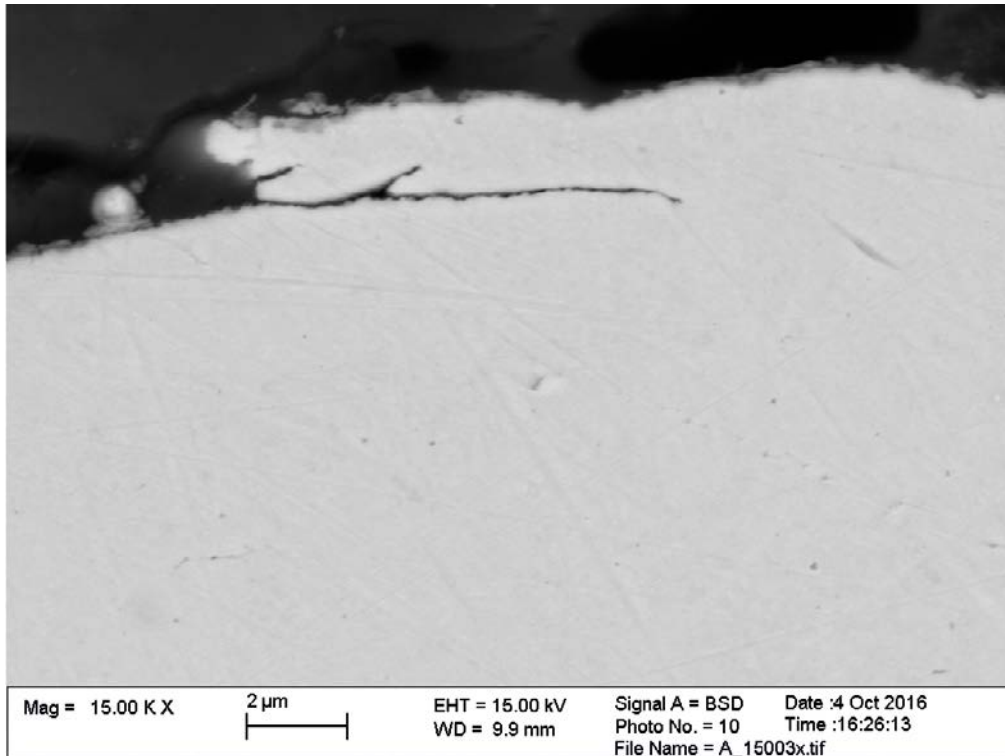


*Figure 3-12. Surface profile showing defects in the surface of sample A.*

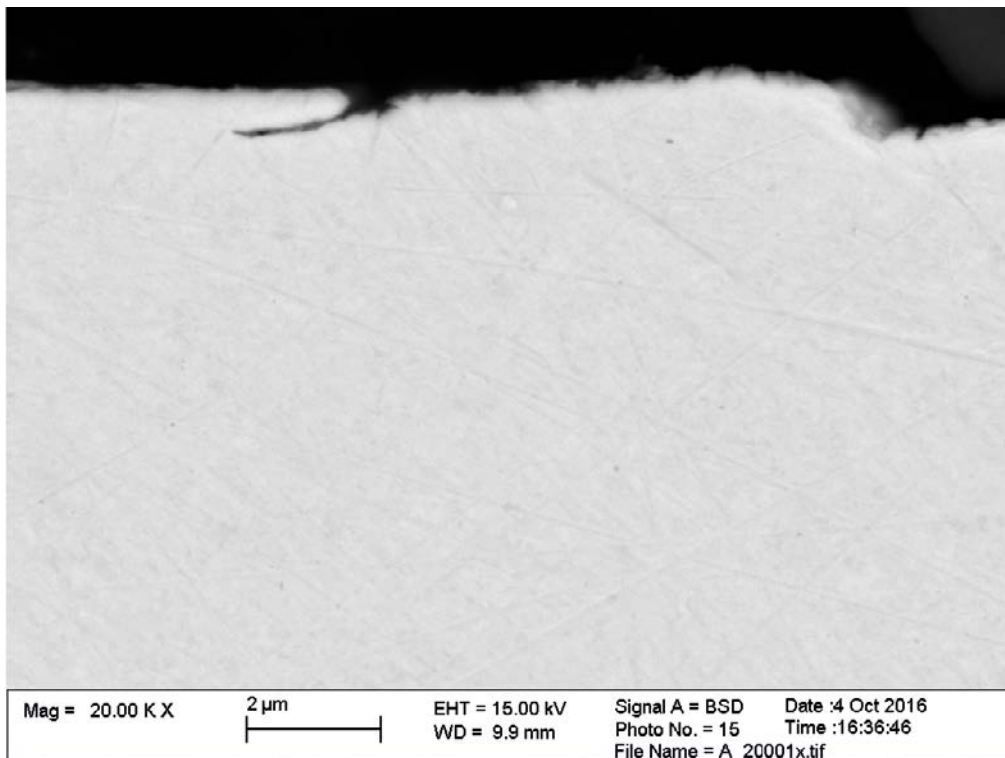


*Figure 3-13. Surface profile showing defects in the surface of sample A.*

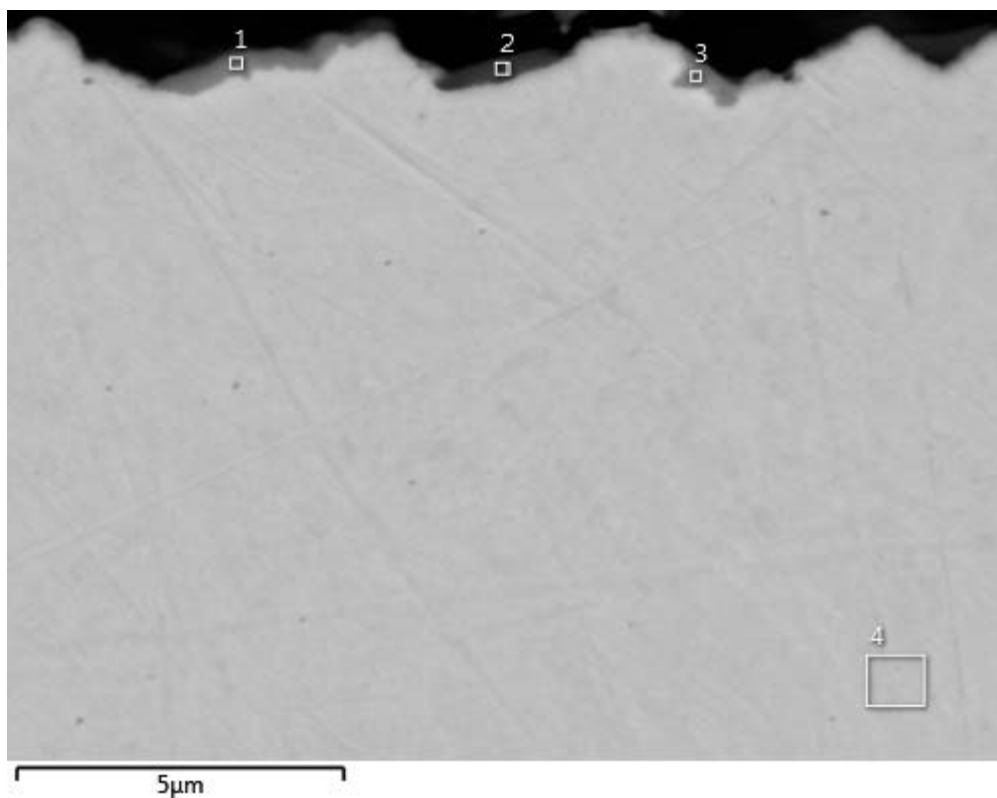


*Figure 3-14. Surface profile with wave like shape on sample A. The areas in the squares in the figure have been analysed with EDS, results are given in Table 3-1.*

**Table 3-1. Elemental composition for the areas indicated in Figure 3-14.**

Element (wt%)	1	2	3	4
C	14.68	21.61	21.48	3.69
O	6.50	9.55	6.97	0.22
Al	0.19	0.21	0.09	0.08
Si	0.09	0.29	0.18	
S		0.05	0.06	
Cl	0.71	0.14	0.85	
Ca	0.09	0.16	0.12	0.09
Fe		0.17		
Cu	75.46	63.91	66.75	95.91
Zn	2.28	3.92	3.50	
Total:	100.00	100.00	100.00	100.00

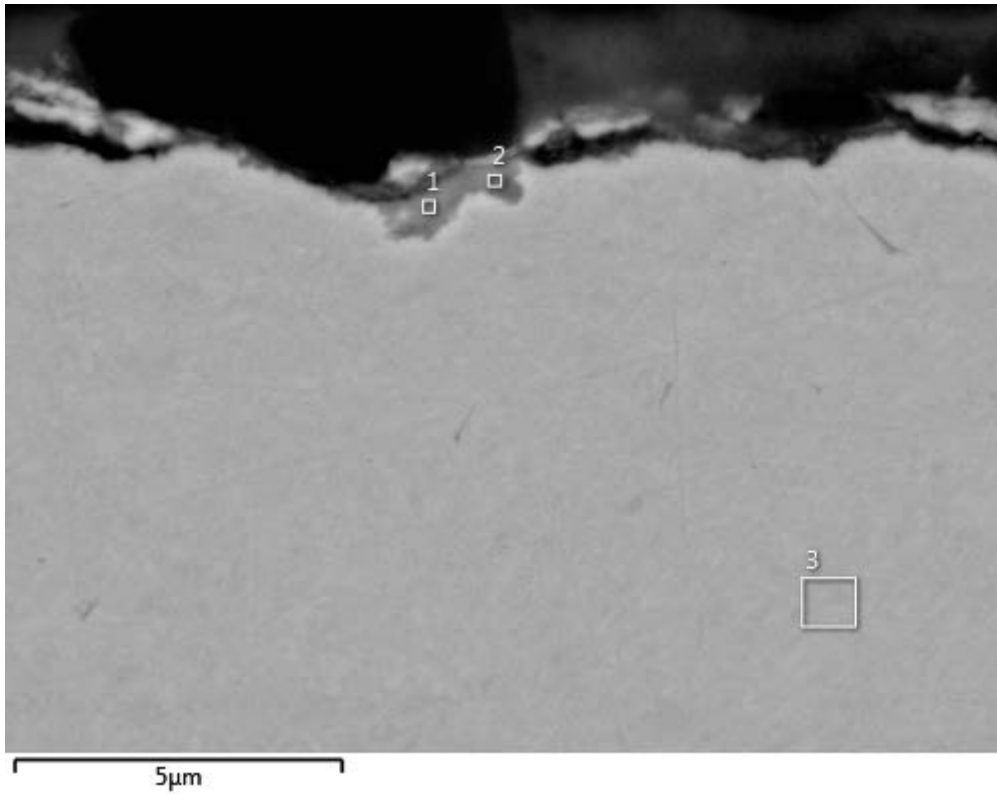


**Figure 3-15.** Surface profile showing corrosion attack with increased oxygen content on sample A. The areas in the squares in the image have been analysed with EDS, results given in Table 3-2.

**Table 3-2. Elemental composition in areas indicated in Figure 3-15.**

Element (wt%)	1	2	3
C	6.67	7.20	3.80
O	8.20	9.18	0.21
Al	1.67	1.98	
Si	0.19	0.20	
S	0.24	0.32	
Cl	1.32	1.26	
Cu	81.72	79.86	95.99
Total:	100.00	100.00	100.00

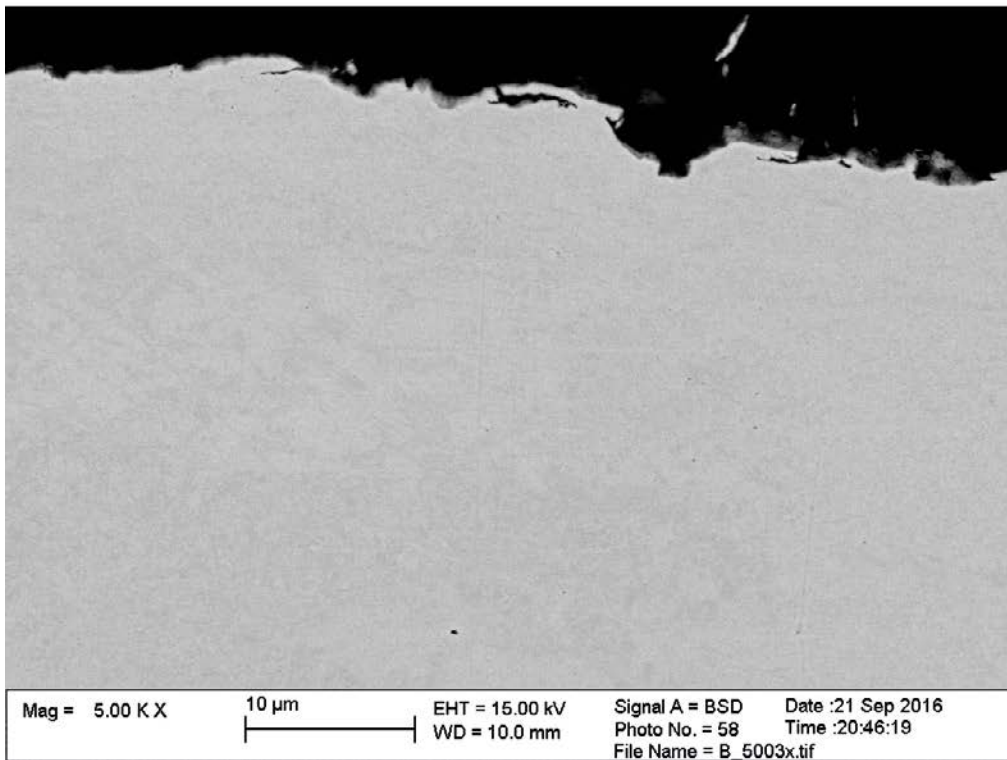
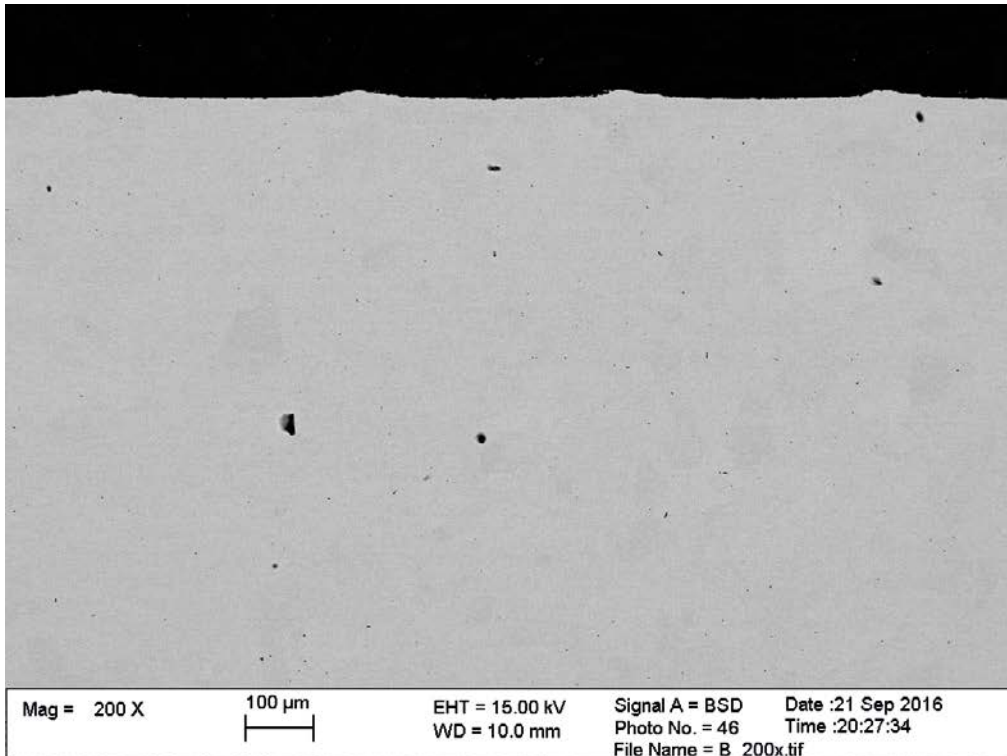


*Figure 3-16. Surface profile for sample B at different magnifications.*



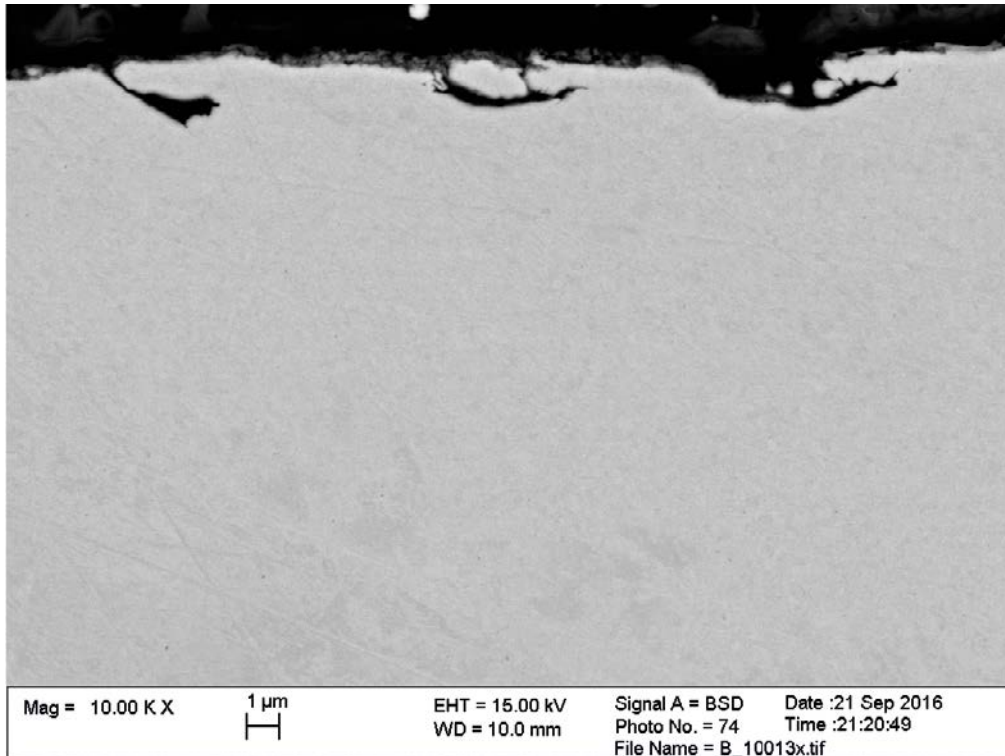


**Figure 3-17.** Surface profile for sample B.

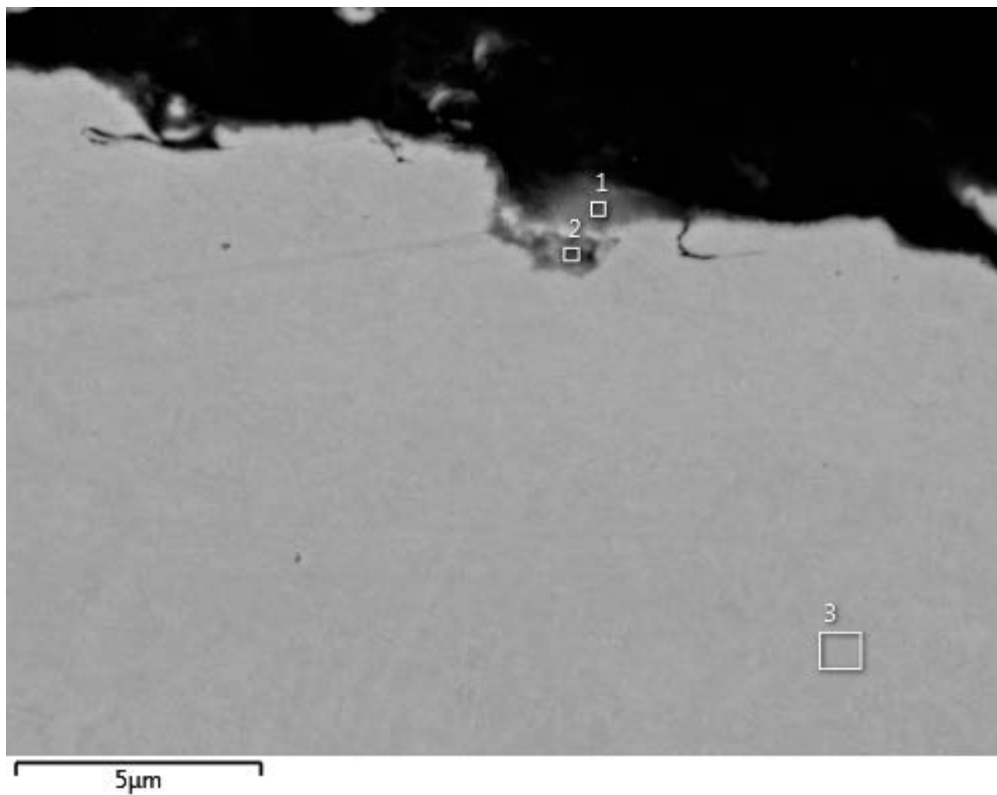


**Figure 3-18.** Surface profile at large magnification for sample B with possible corrosion attack. The areas in the squares in the image have been analysed with EDS and the result is shown in Table 3-3.

**Table 3-3. Elemental composition for areas indicated in Figure 3-18.**

Element (wt%)	1	2	3
C	17.21	10.96	3.84
O	4.63	3.51	0.22
Mg	0.24	0.19	
Al	0.42	0.27	
Si	0.11		
Cl	0.13	0.14	
Ca	0.14		
Cu	72.96	82.25	95.94
Zn	4.16	2.67	
Total:	100.00	100.00	100.00

**Table 3-4. Elemental composition for areas indicated in Figure 3-19.**

Element (wt%)	1	2	3
C	23.93	24.69	4.26
O	5.25	6.72	0.24
Al	1.30	1.55	
Si	0.83	0.66	
S	0.10		
Cl	0.26	0.25	
Ca	0.36	0.32	
Ti	0.21		
Cu	67.77	65.80	95.50
Total:	100.00	100.00	100.00

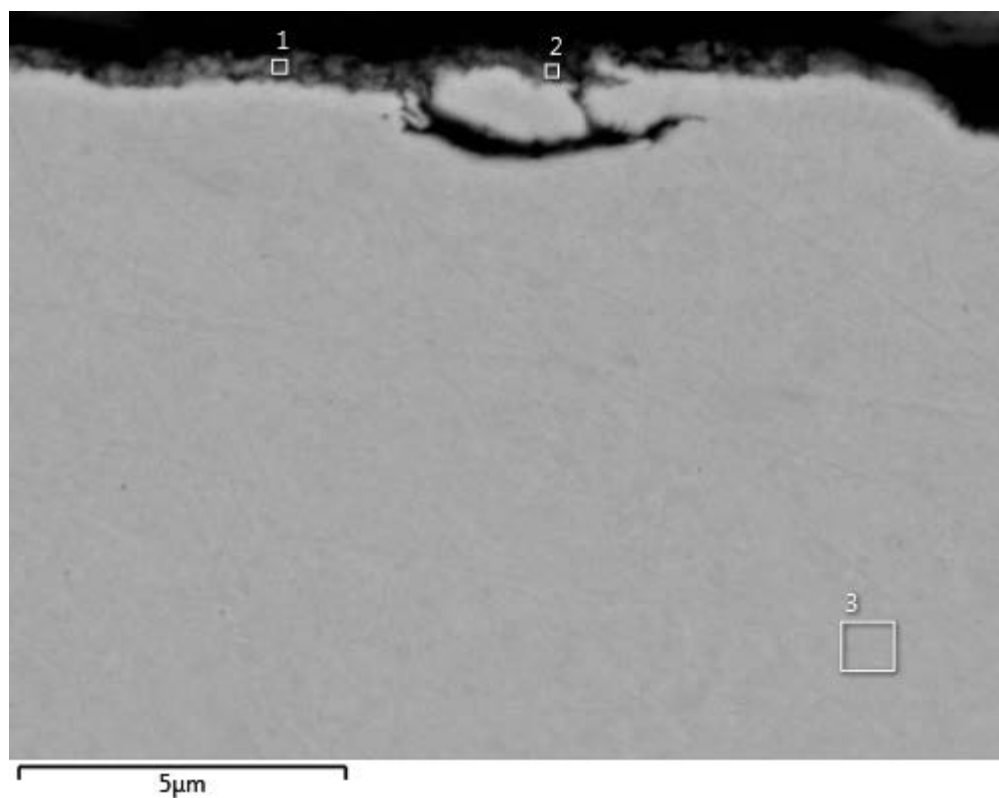


**Figure 3-19.** Surface profile at large magnification, sample B. The areas in the squares in the image have been analysed with EDS and the result are given in Table 3-4.



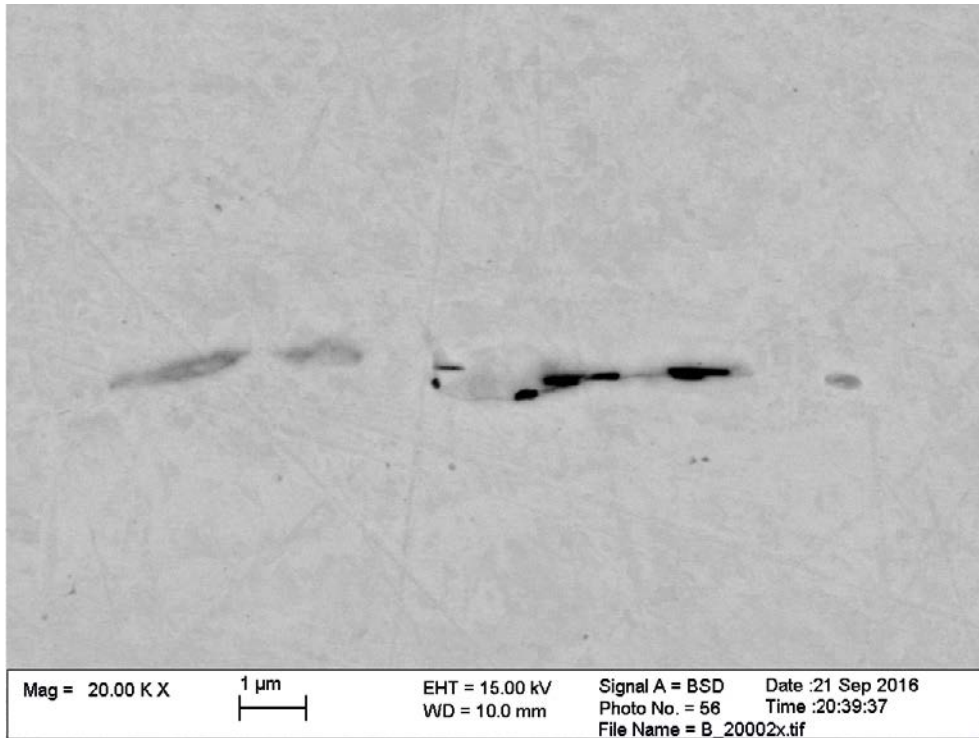


*Figure 3-20. Possible contamination or cavity in the bulk of sample B.*

### 3.3 EDS mapping

Photos from EDS mapping are shown in Figure 3-21 to Figure 3-24. Figure 3-21 and Figure 3-23 show SEM backscatter images of the surface. In Figure 3-22 and Figure 3-24, the EDS detector has been used to obtain the elemental composition at the surface of the analyzed area.

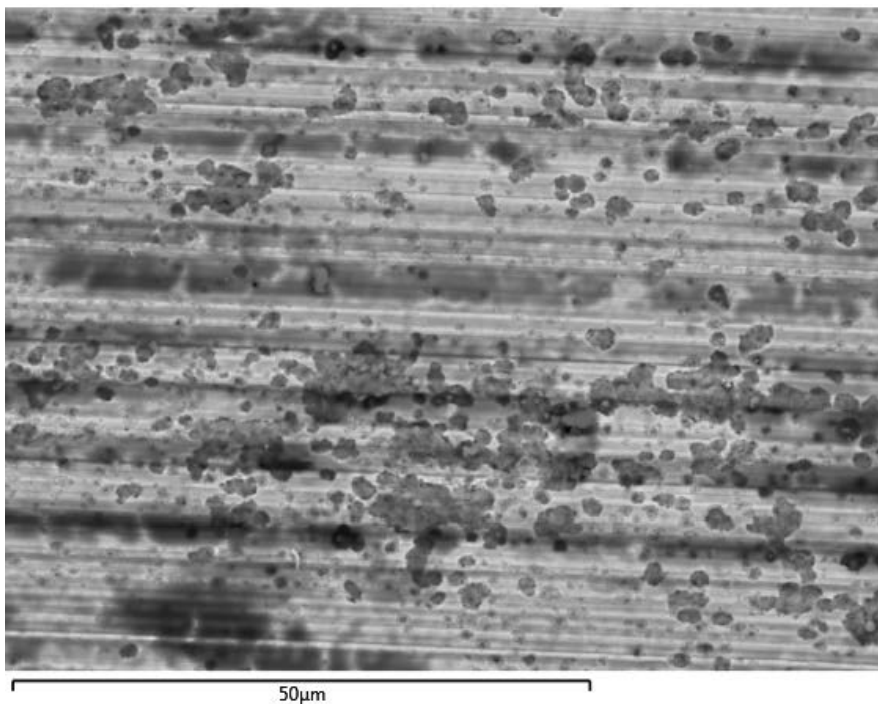


*Figure 3-21. SEM-image over the area that has been mapped with EDS, sample A.*

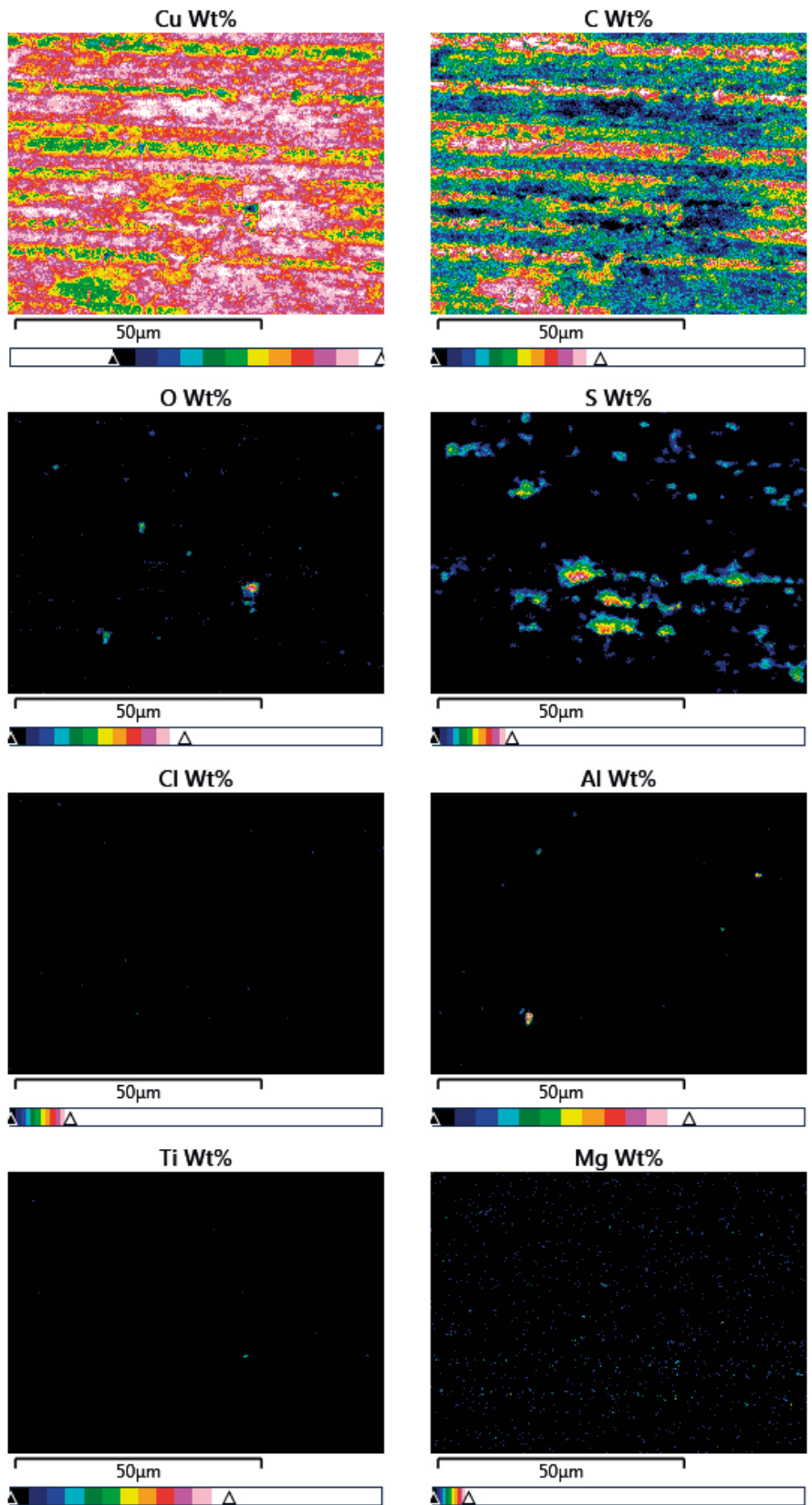
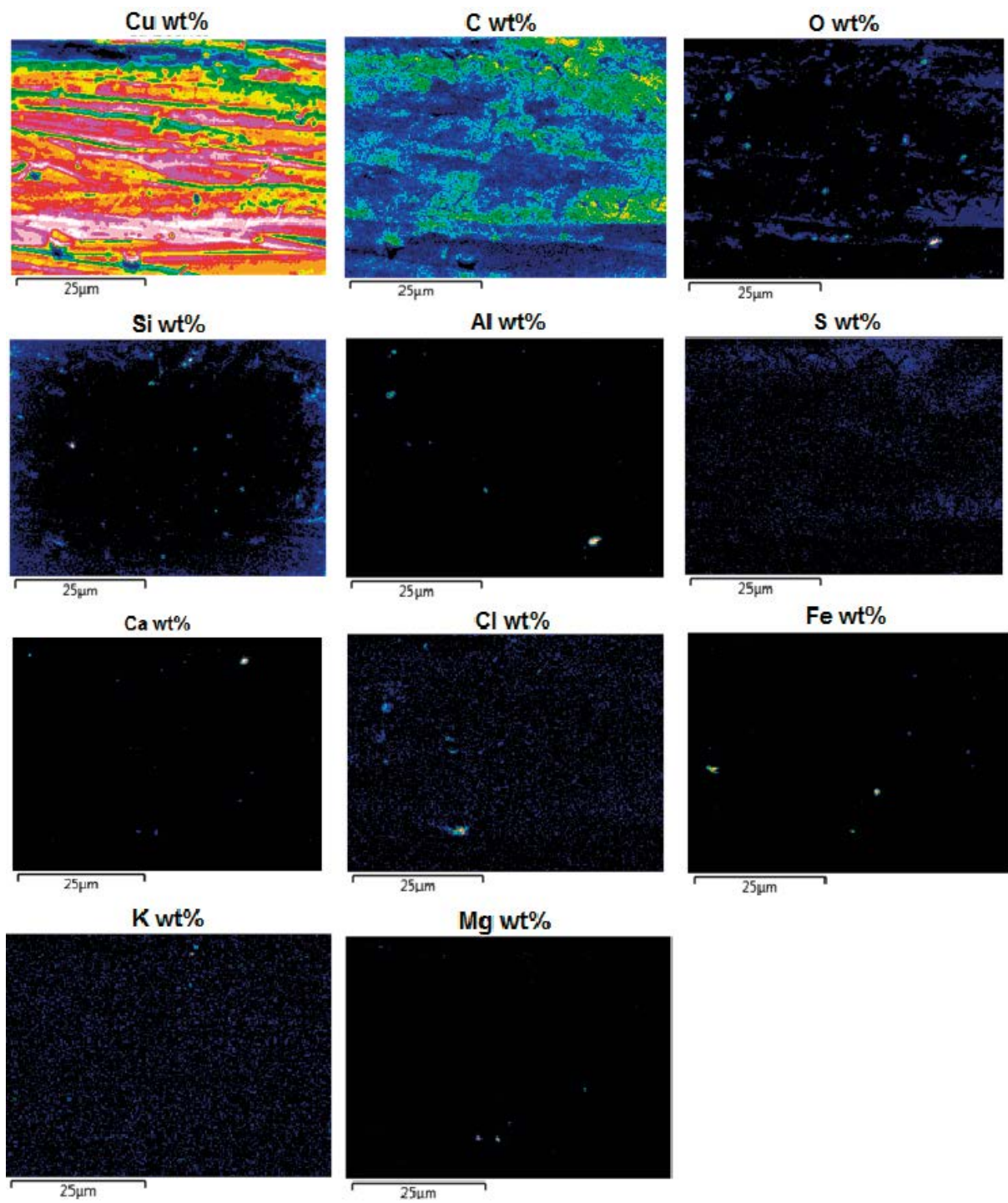


Figure 3-22. Results from EDS mapping over the surface in Figure 3-21.



*Figure 3-23. SEM image over the area that has been mapped with EDS, surface B.*



*Figure 3-24. EDS mapping over the surface in Figure 3-23.*

### 3.4 GD-OES analysis

Depth profiles showing the elemental composition are shown in Figure 3-25 to Figure 3-32. For each sample, one surface analysis is made with a sputter depth of 40  $\mu\text{m}$ . The result is presented in graphs with different values on the axes.

The content of carbon, oxygen and hydrogen in the surface region was obtained from the GD-OES software and is presented in Table 3-5. The content is corresponding to the sputtered depth in the sample but is presented as the content corresponding to the analyzed surface area in  $\text{g}/\text{m}^2$ . Data from two samples from Taxén et al. (2012) are also included in the table, denoted Prototype sample 1 and 2. In the previous report these corresponds to GD-OES samples denoted “delprov 1” and “delprov 2”.

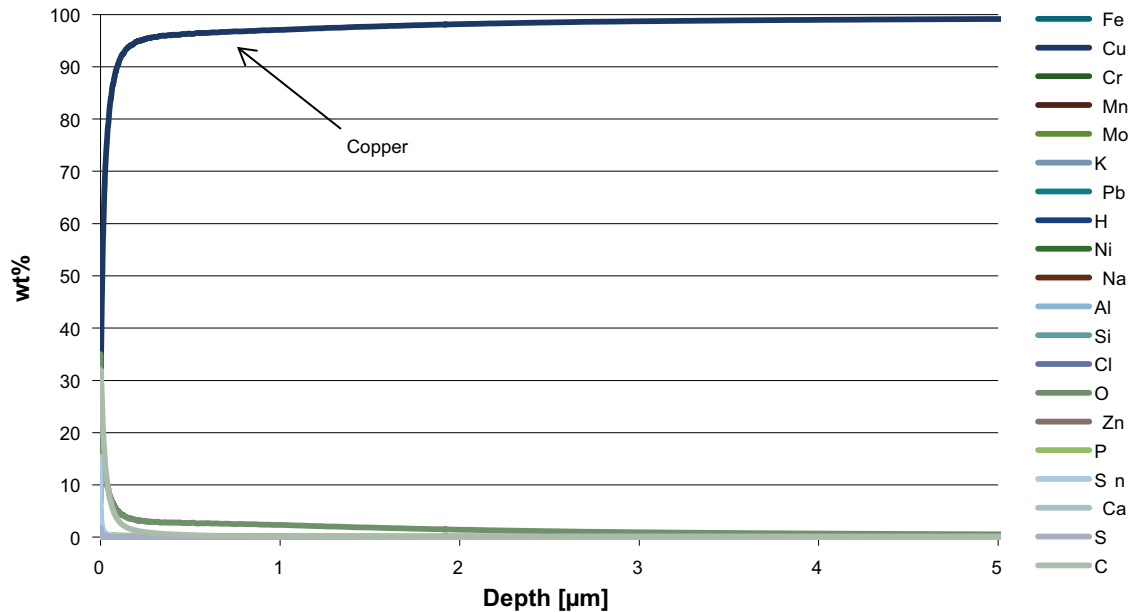


Figure 3-25. Elemental composition vs sputter depth for sample A.

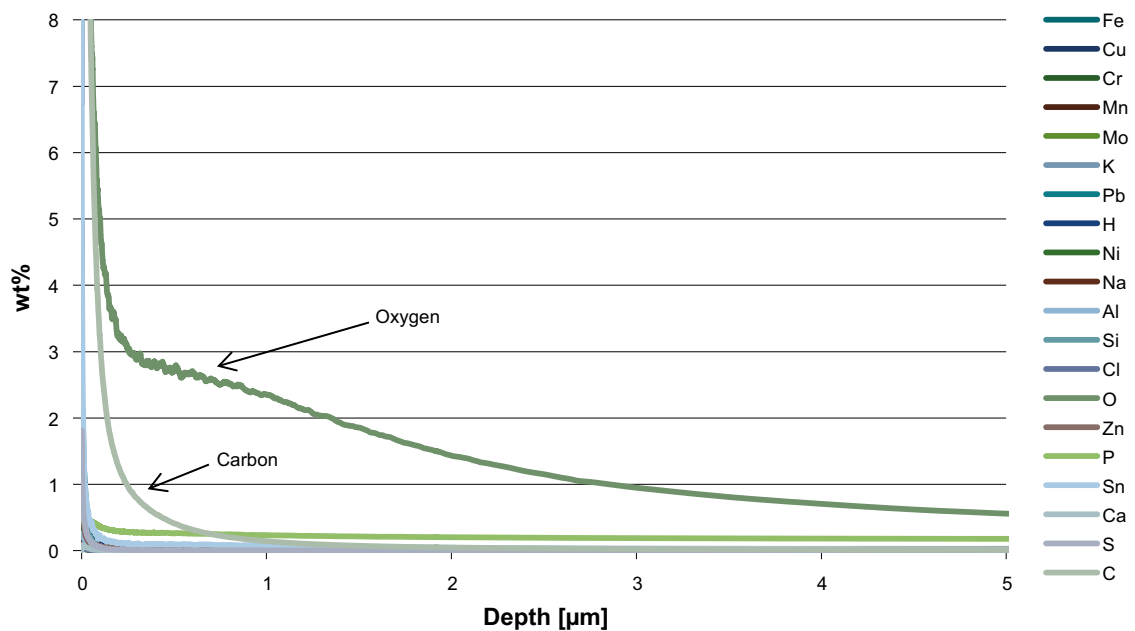


Figure 3-26. Detail of Figure 3-25 sample A.

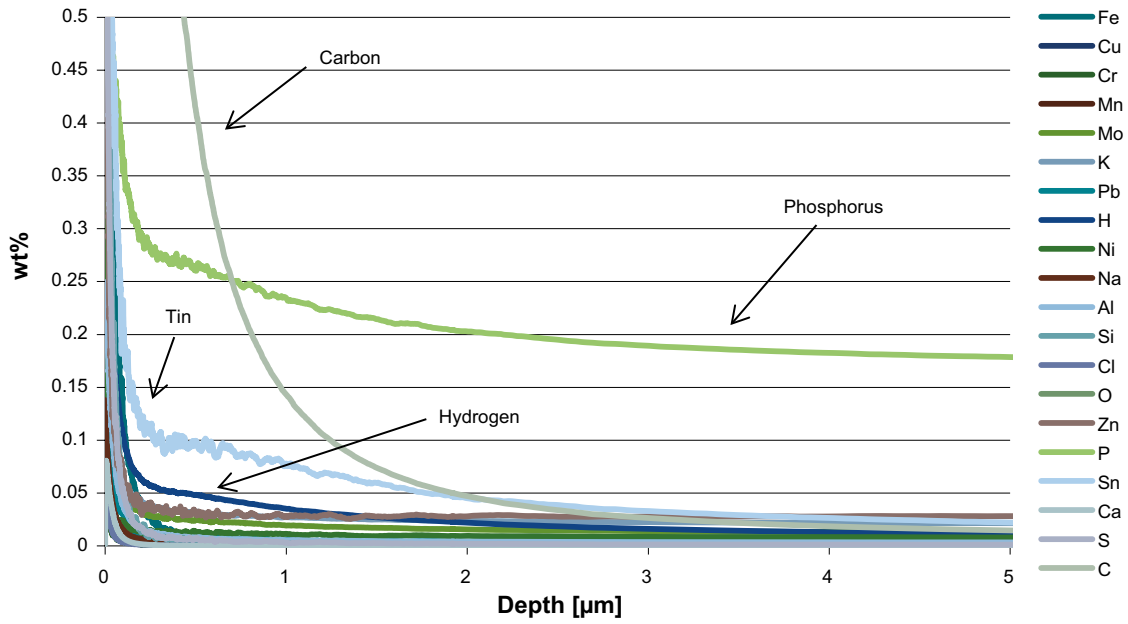


Figure 3-27. Detail of Figure 3-26, sample A.

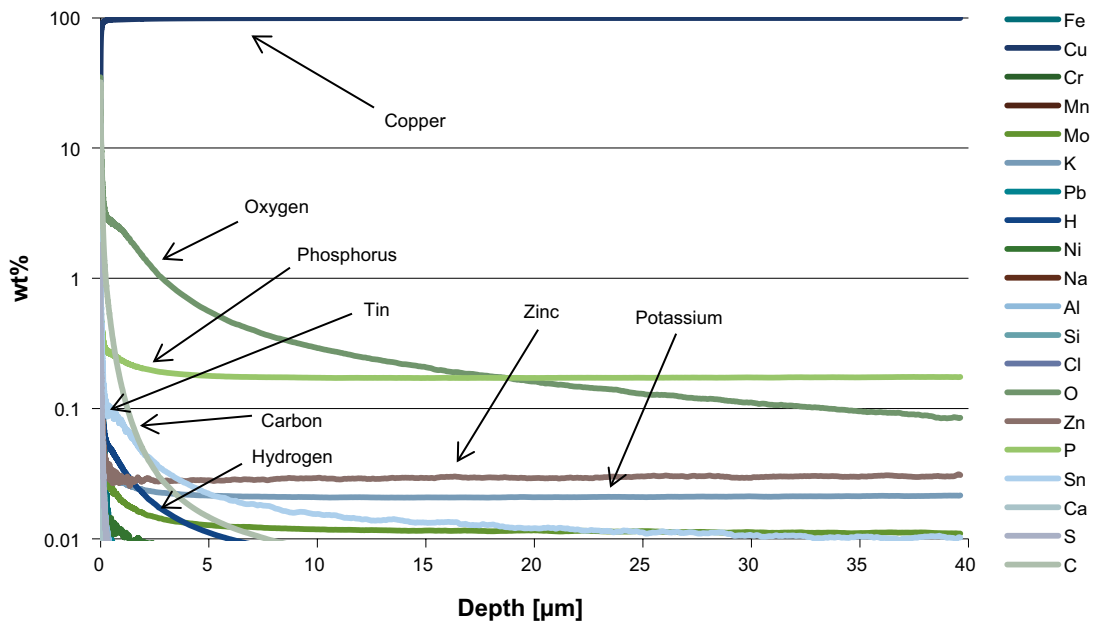


Figure 3-28. Elemental content shown with a logarithmic scale, sample A.



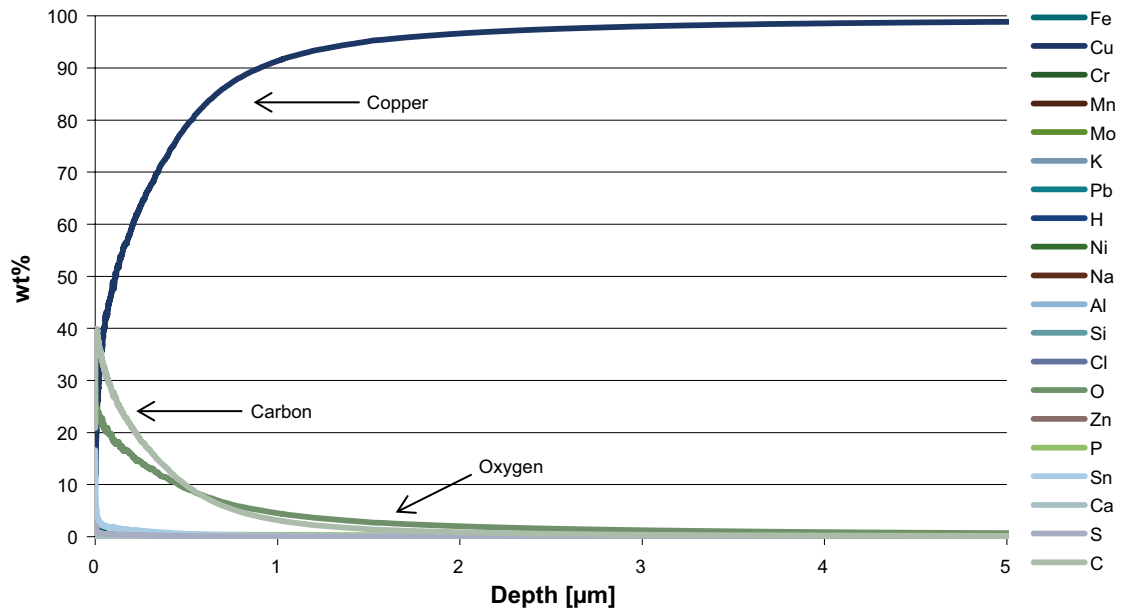


Figure 3-29. Elemental composition vs sputter depth for sample B.

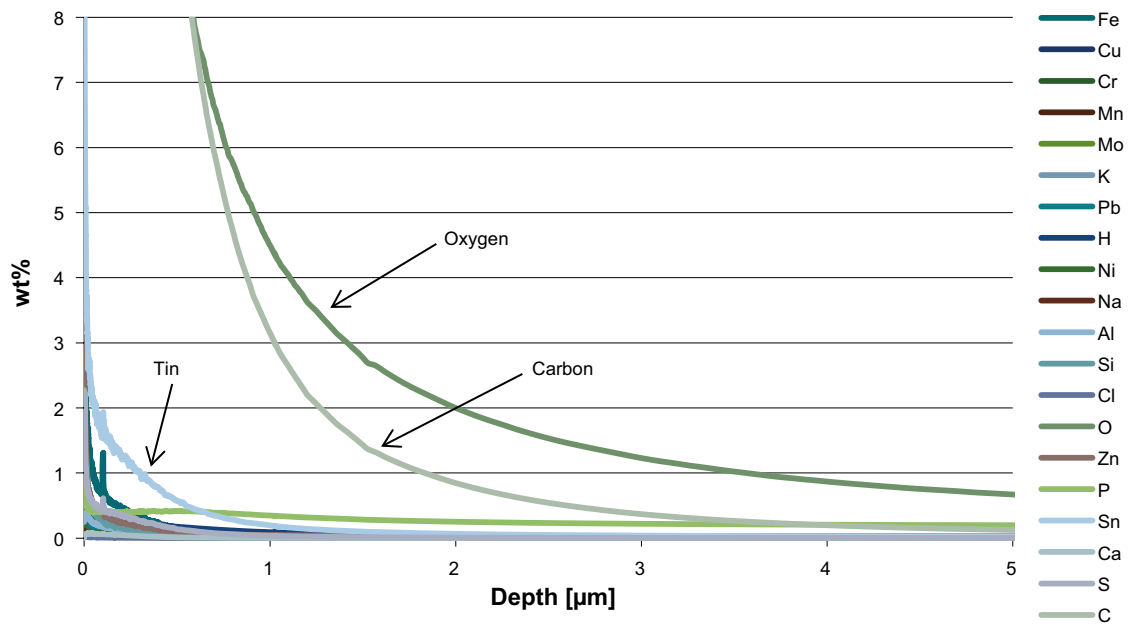


Figure 3-30. Detail of Figure 3-29, sample B.

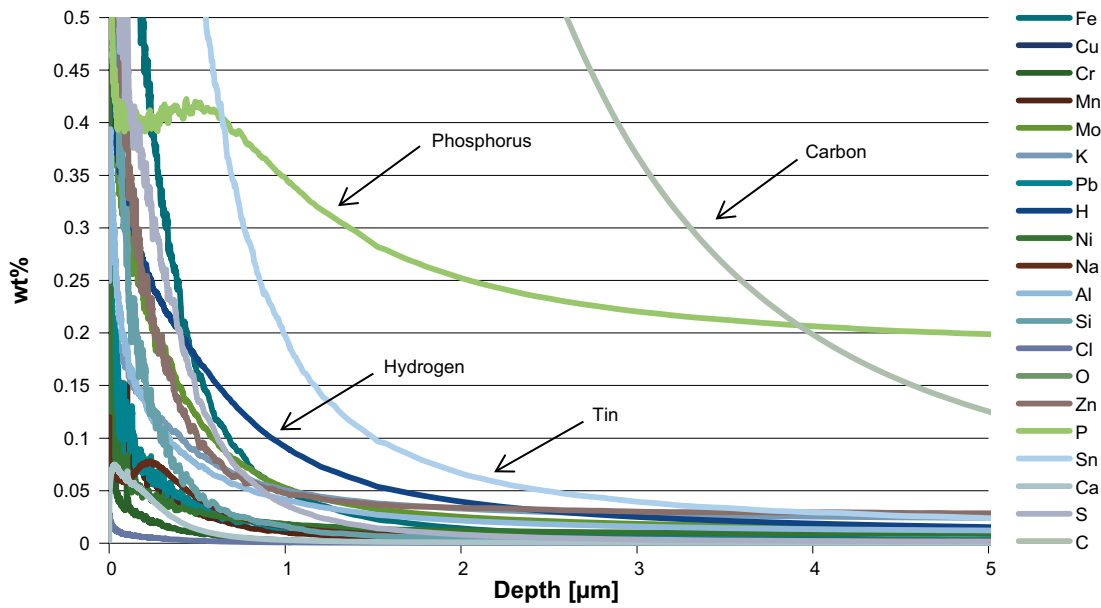


Figure 3-31. Detail of Figure 3-30, sample B.

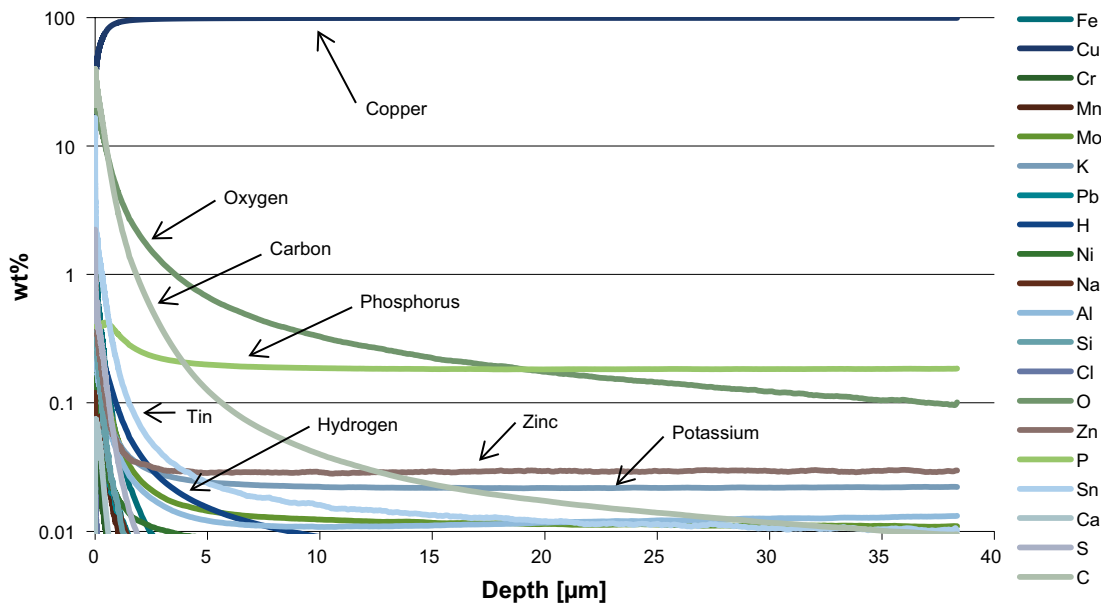


Figure 3-32. Elemental content shown with a logarithmic scale, sample B.

Table 3-5. Comparison of surface elemental composition regarding C, O, and H in the samples A and B, with samples from the Prototype repository.

Sample	Depth [ $\mu\text{m}$ ]	C [ $\text{g}/\text{m}^2$ ]	O [ $\text{g}/\text{m}^2$ ]	H [ $\text{g}/\text{m}^2$ ]
Cu A	10	0.114	0.807	0.015
Cu A	6	0.110	0.679	0.012
Cu A	2.5	0.105	0.465	0.008
Cu B	10	0.859	1.246	0.025
Cu B	6	0.838	1.100	0.022
Cu B	2.5	0.773	0.839	0.016
Prototype sample 1	10	0.686	4.405	0.022
Prototype sample 2	10	0.564	3.499	0.022



## 4 Discussion

Traces from the mechanical processing and handling of the material can be seen for both samples examined. Numerous deposits are visible with a thickness up to 13  $\mu\text{m}$ .

From the metallographic examination of both samples it can be seen that the grains close to the surface do not differ from the bulk. No intercrystalline cracks could be distinguished.

In cross sections of the samples, pits and defects of around 1  $\mu\text{m}$  occurred frequently. The deepest pit found on sample A was about 3  $\mu\text{m}$  deep. Both samples A and B show cracks that are a few  $\mu\text{m}$  deep and that are present close to the surface, see Figure 3-12 and Figure 3-17. These cracks are believed to have formed during mechanical processing of the surface.

Sample A shows an area where the surface profile is wavy, possibly due to the mechanical machining of the copper tubes (see Figure 3-14). EDS analysis in the valleys show levels of oxygen of up to 9.5 wt%, reflecting atmospheric corrosion of the surface. Similar, but slightly lower levels of oxygen were found in areas analyzed on sample B.

The high level of carbon close to the surface, varying between 7 and 25 wt% between the areas analyzed may come from the metallographic mounting material Konductomet which contains carbon, but may also come from dust and particles deposited during the long storage period. For example, at the surface profile for sample B, seen in Figure 3-17 and Figure 3-19, a thin layer can be seen, thinner than 1  $\mu\text{m}$ . This layer contains large amounts of carbon and is believed to have formed during sample preparation.

Small amounts of aluminum, silicon, calcium and iron are also present in the valleys. Zinc at levels of up to 4 wt% was present on both samples.

The EDS mapping performed show the presence of various elements on the surface. On sample A, an area with a few shallow pits has been studied, see Figure 3-21. Carbon is present in a striped pattern on the surface, see Figure 3-22. Oxygen is indicated only as spots which indicates that the surface has not generally been oxidized. Sulfur and chlorine are indicated, chlorine only as one spot. Small amounts of aluminum, titanium and magnesium are also identified on the surface.

From the EDS mapping on sample B it can be seen that carbon is present in high amounts, see Figure 3-24. Oxygen is present to some extent, with higher intensity in a number of areas. Small amounts of sulfur are present over the examined surface. Chlorine is also present to some extent, with a higher intensity in a number of areas. Potassium, silicon, aluminum, iron and magnesium were also identified on the examined surface.

The GD-OES analysis of sample A shows mainly oxygen and carbon at the surface. The oxidation depth is about 1–1.5  $\mu\text{m}$ . The “tail” of the oxygen profile in Figure 3-25 to Figure 3-32 is a GD-OES artefact, not reflecting the actual oxygen level. Some hydrogen could be detected within the first  $\mu\text{m}$ . Phosphorus is present at the surface but the concentration is not as high as presented in the graphs a few  $\mu\text{m}$  into the material. With the GD-OES method used, phosphorus in copper gives a higher signal than corresponding to the true composition since the method is not independent of the base metal, differing slightly from the standard materials used for calibration. The tin values are also higher than the true composition due to the plasma not being stable during the absolute first part of the measurement (~0.1–0.2 s).

For sample B, oxygen and carbon are also clearly present. Hydrogen is present at the surface within the first  $\mu\text{m}$ . Here too, the phosphorus content is higher than the actual value as well as the tin. Because of the texture on the surface of sample B, the connection between the sample and the o-ring of the GD-OES instrument was probably not completely tight. Due to, this, some air probably leaked into the instrument, resulting in higher oxygen content than the true value.

Since the samples for EDS-mapping and GD-OES samples were not mounted in metallographic resin, the carbon content cannot be related to the mounting material. The copper surfaces have thus been contaminated with carbon from another source.

The GD-OES data obtained for samples A and B can be compared to data obtained for samples taken from the copper canisters of the Prototype repository (Taxén et al. 2012). As Table 3-5 shows, the elemental contents of C, O, and H was integrated for the sputter depths 2.5, 6 and 10  $\mu\text{m}$  for the samples A and B, while the corrosion of the surface of the Prototype canisters made it meaningful only to analyze the content at 10  $\mu\text{m}$  depth. A comparison shows that while the oxygen content is 3–4 times higher at 10  $\mu\text{m}$  depth in the samples from the Prototype canisters, the amount of hydrogen in the Prototype samples were similar but in fact intermediate between the samples A and B.

## 5 Conclusion

Traces from mechanical processing are visible on the surface of both samples examined. There are a few  $\mu\text{m}$  deep crack-like surface defects almost parallel to the surface on both samples analyzed. Pits and pit-like defects of up to about 3  $\mu\text{m}$  depth occurred on the surfaces of the samples. EDS analysis has shown a contaminated surface with presence of carbon, sulfur and, to some extent, chlorine. GD-OES depth analyses mainly revealed oxygen and carbon at the surface. Some hydrogen could be detected within the first few  $\mu\text{m}$ .



## References

SKB's (Svensk Kärnbränslehantering AB) publications can be found at [www.skb.se/publications](http://www.skb.se/publications).

**Taxén C, 2013.** Ytprofiler på kopparkapslar från deponeringshål 5 och 6 i försöksserien Prototyp. SKB P-13-50, Svensk Kärnbränslehantering AB. (In Swedish.)

**Taxén C, Lundholm M, Persson D, Jakobsson D, Sedlakova M, Randelius M, Karlsson O, Rydgren P, 2012.** Analyser av koppar från prototypkapsel 5 och 6. SKB P-12-22, Svensk Kärnbränslehantering AB. (In Swedish.)



Additional photos

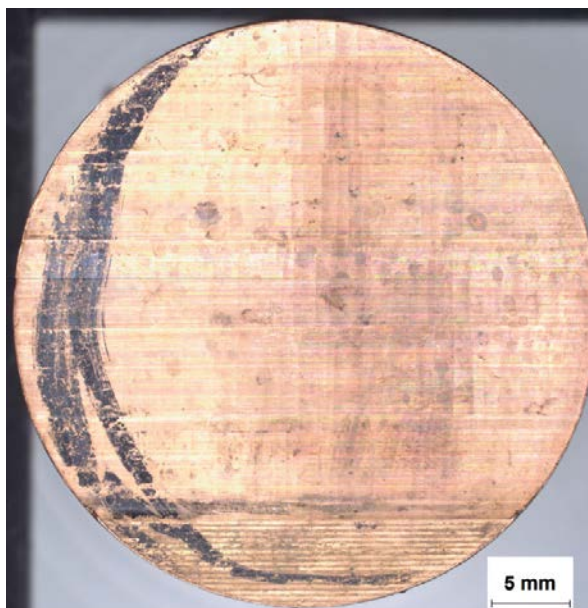


Figure A-1. Overview image of sample A.

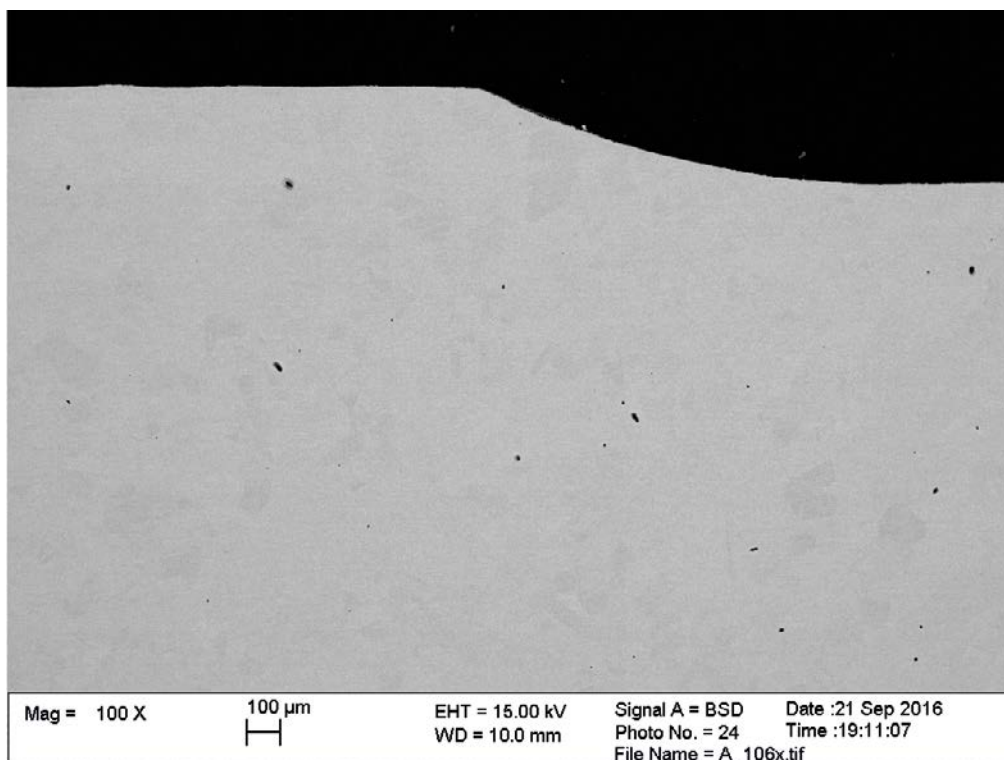
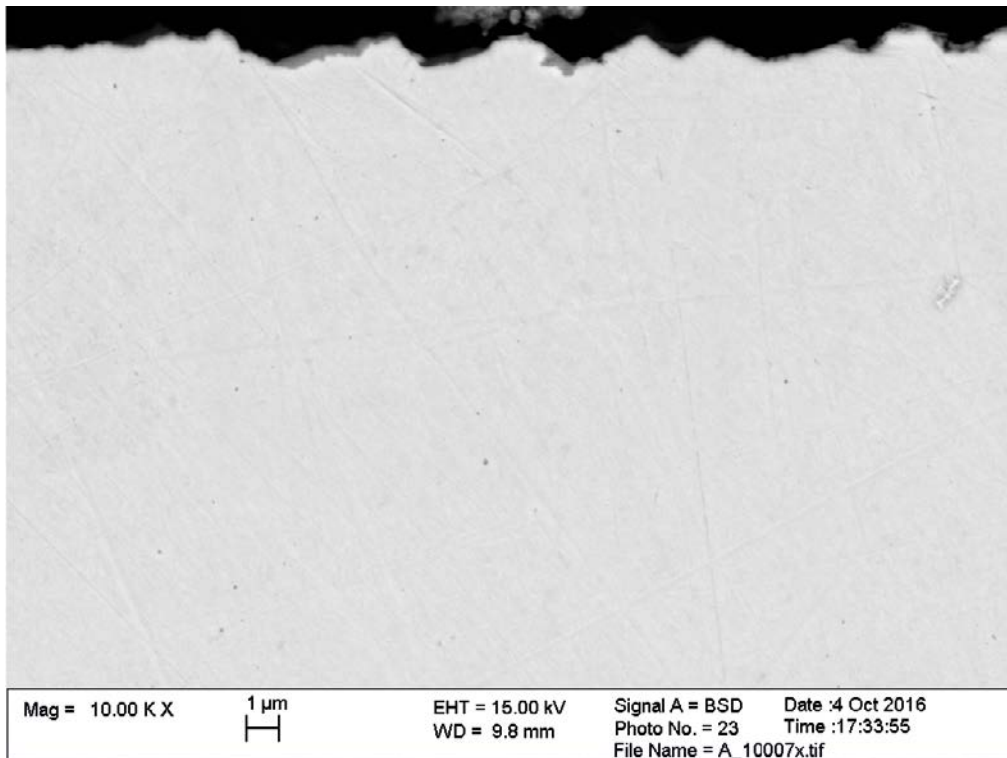
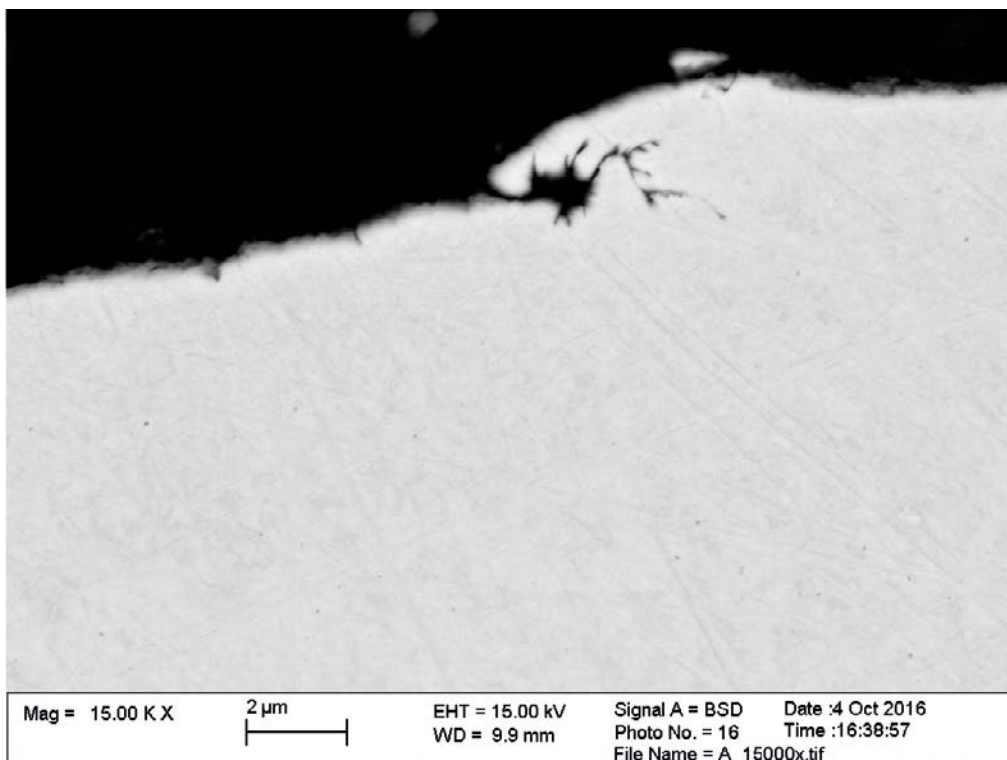


Figure A-2. Transition between the two different areas that can be distinguished in Figure A-1.



*Figure A-3. Surface profile of sample A.*



*Figure A-4. Surface profile of sample A.*



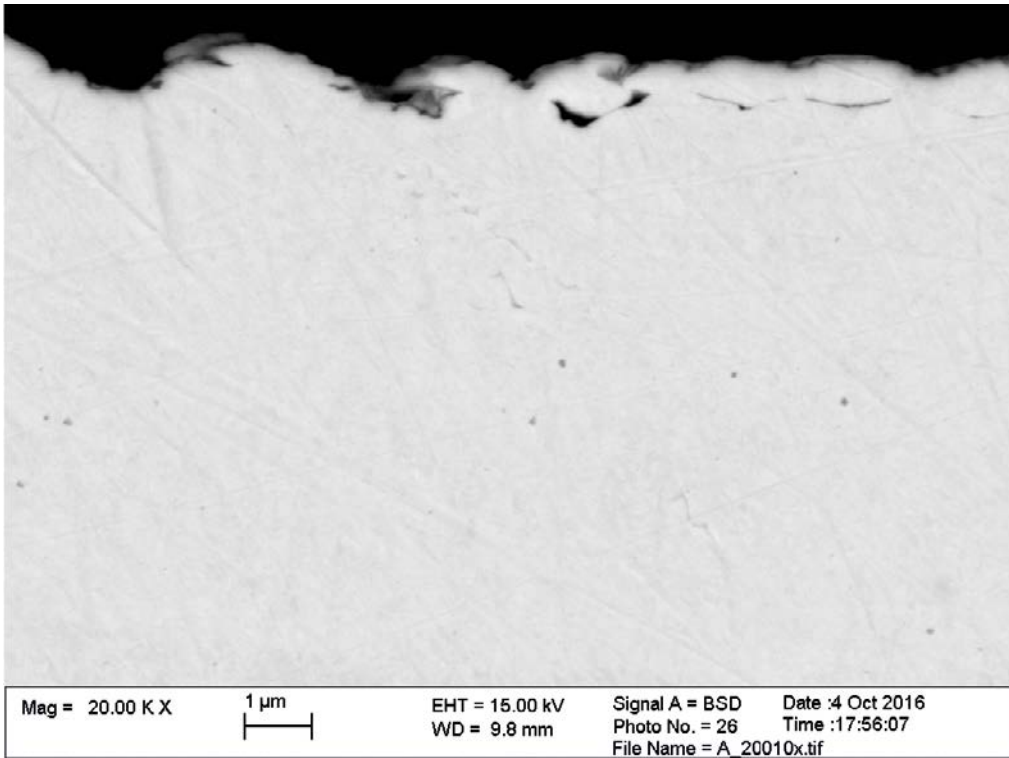


*Figure A-5. Surface profile of sample A.*

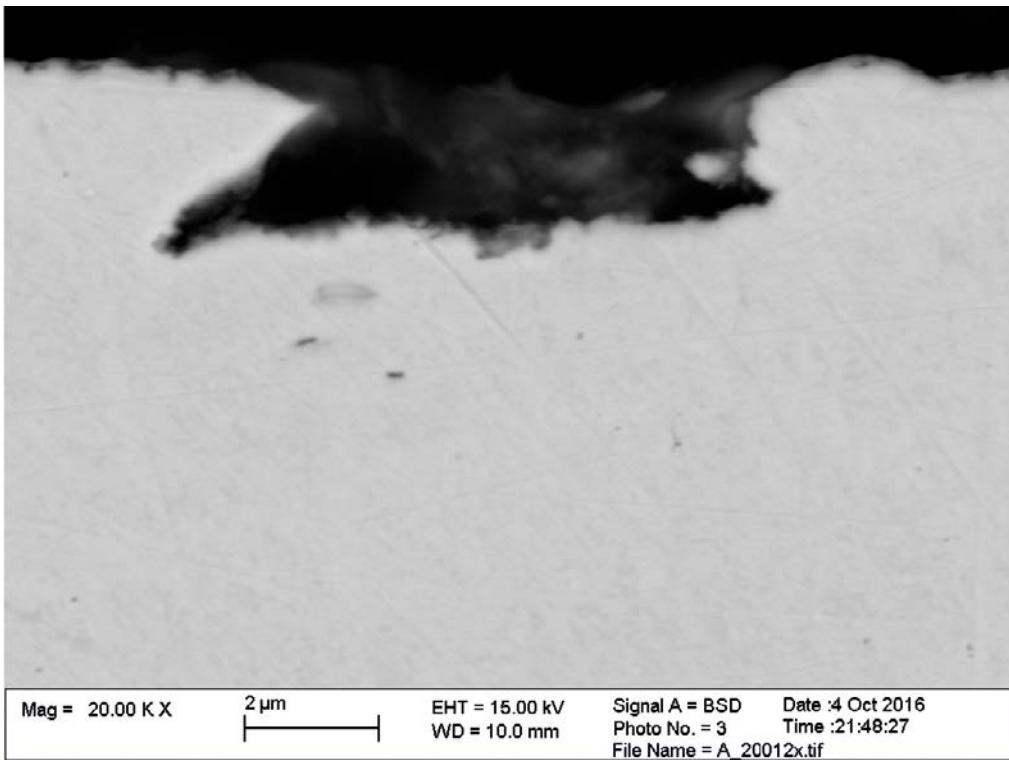


*Figure A-6. Surface profile of sample A.*

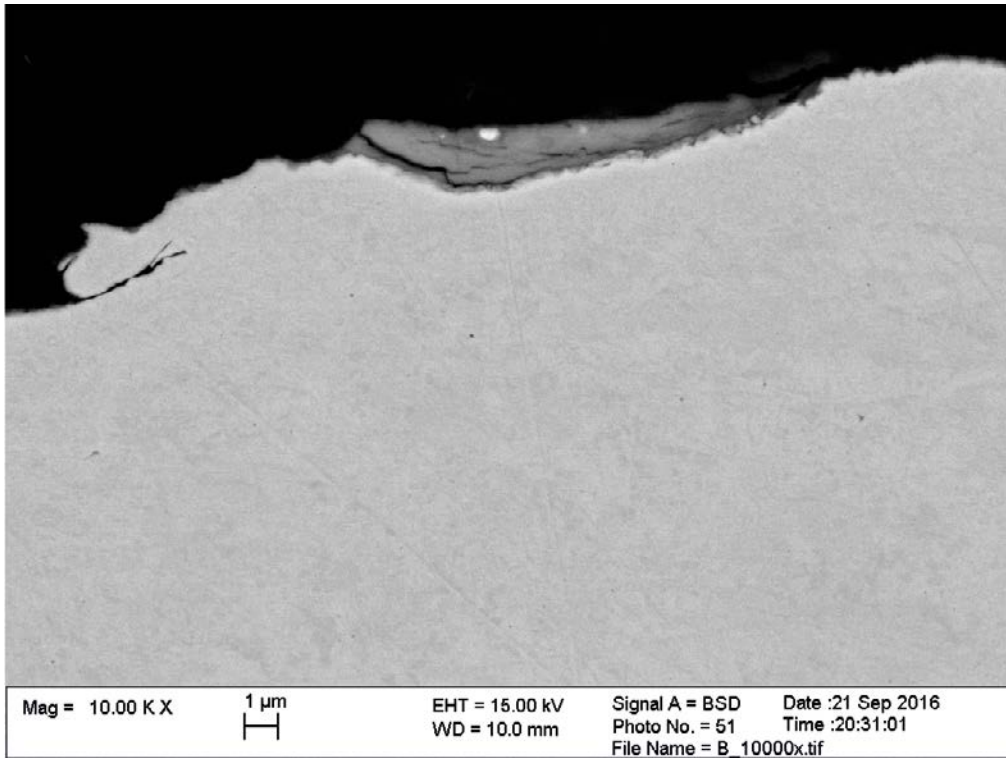


*Figure A-7. Surface profile of sample B.*

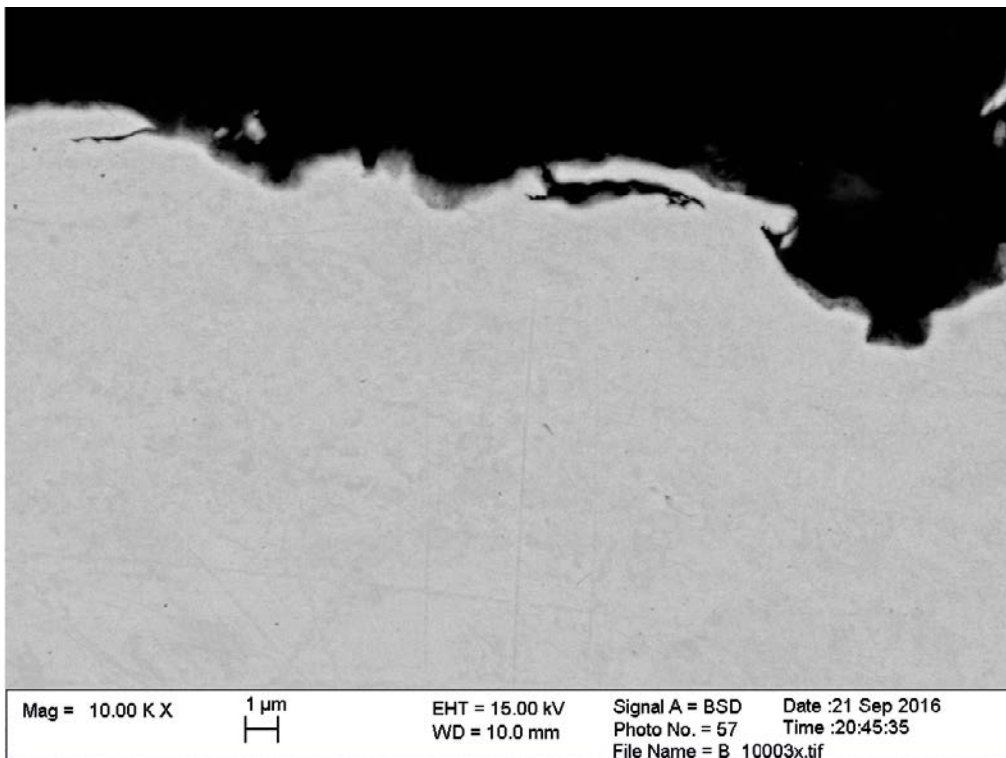


*Figure A-8. Surface profile of sample B.*

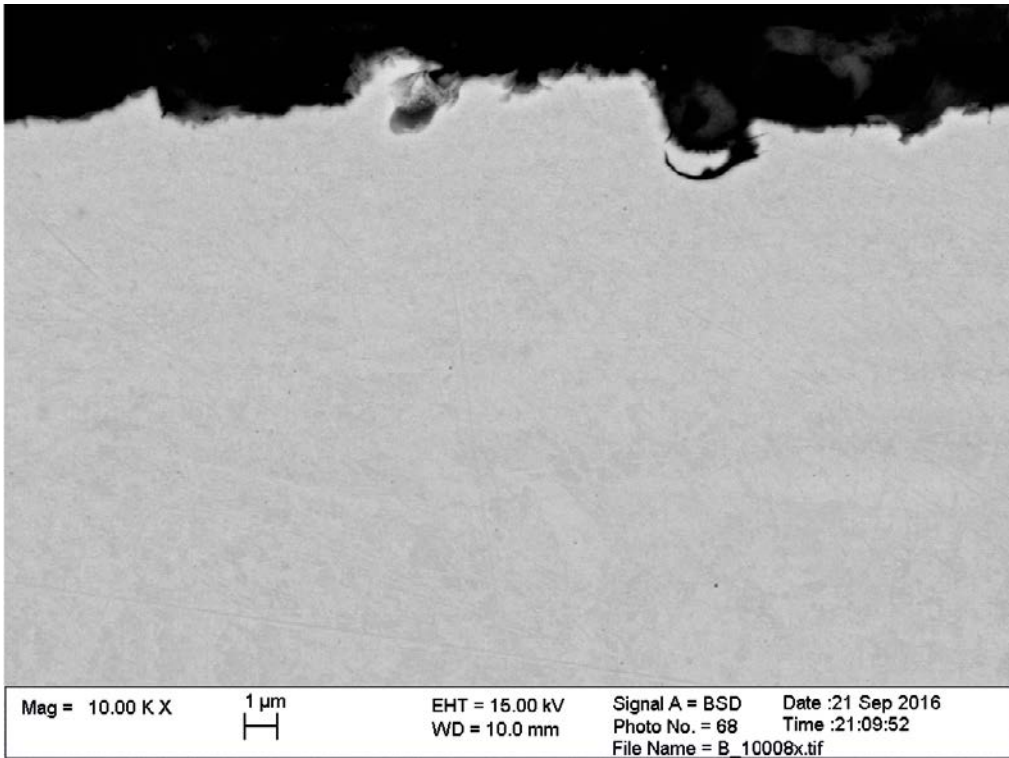


*Figure A-9. Surface profile of sample B.*

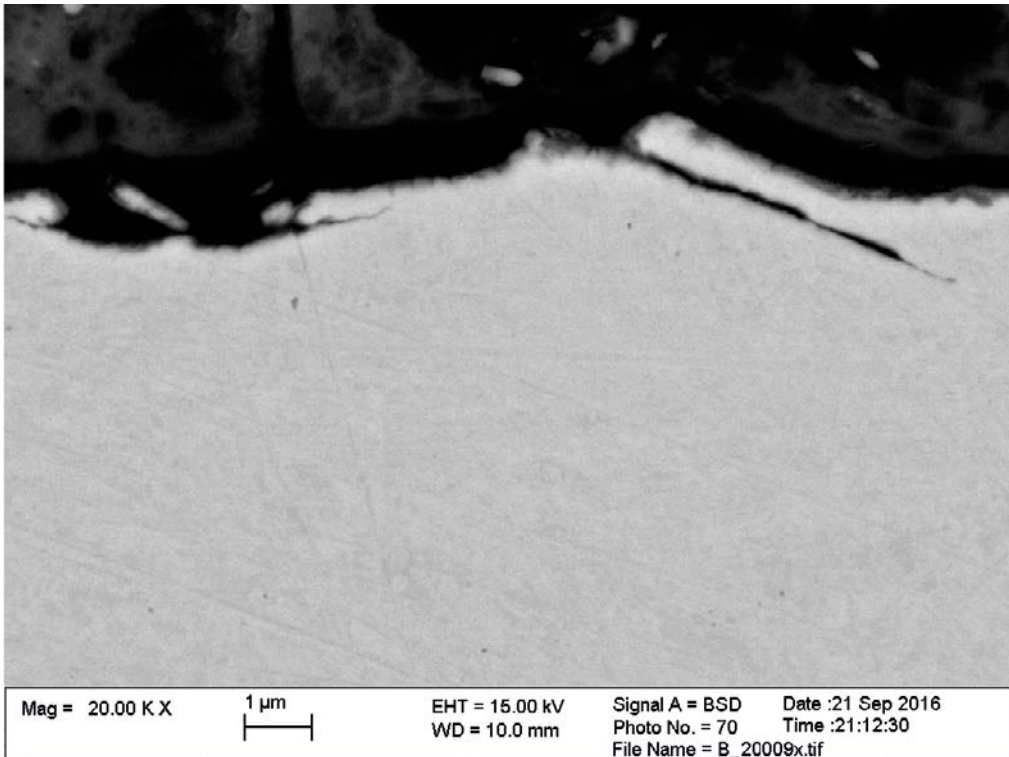


*Figure A-10. Surface profile of sample B.*

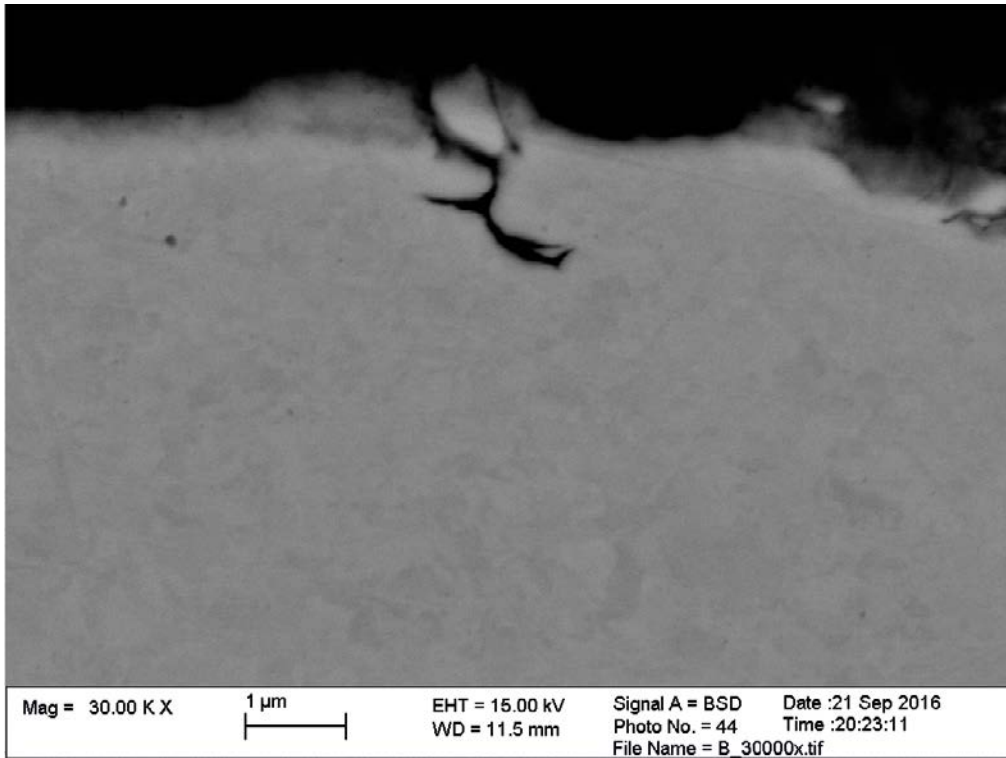


*Figure A-11. Surface profile of sample B.*

SKB is responsible for managing spent nuclear fuel and radioactive waste produced by the Swedish nuclear power plants such that man and the environment are protected in the near and distant future.

**skb.se**